

Low-energy spectra of nobelium isotopes: Skyrme random-phase-approximation analysis

V.O. Nesterenko ^{1,2}, M.A. Mardyban ^{1,2}, A. Repko ³, R.V. Jolos^{1,2}, P.-G. Reinhard ⁴ and Alan A. Dzhioev¹

¹ *Laboratory of Theoretical Physics, Joint Institute for Nuclear Research, 141980, Dubna, Moscow region, Russia*

² *Dubna State University, 141982, Dubna, Moscow region, Russia*

³ *Institute of Physics, Slovak Academy of Sciences, 84511 Bratislava, Slovakia and*

⁴ *Institute for Theoretical Physics II, University of Erlangen, D-91058, Erlangen, Germany*

(Dated: July 29, 2025)

Low-energy spectra in the isotopic chain $^{250-262}\text{No}$ are systematically investigated within the fully self-consistent Quasiparticle Random-Phase-Approximation (QRPA) using Skyrme forces SLy4, SLy6, SkM* and SVbas. QRPA states of multipolarity $\lambda\mu=20, 22, 30, 31, 32, 33, 43, 44$ and 98 are considered. The main attention is paid to isotopes ^{252}No and ^{254}No where the most extensive experimental spectroscopic information is available. In these two nuclei, a reasonable description of $K^\pi = 8^-, 2^-$ and 3^+ isomers is obtained with forces SLy4 and SLy6. The disputed 8^- isomer in ^{254}No is assigned as neutron two-quasiparticle configuration $nn[734\uparrow, 613\uparrow]$. The isomers are additionally analyzed using Skyrme functionals UNEDF1, UNEDF2 and UNEDF1^{SO}. At the energies 1.2 - 1.4 MeV, the 2qp K -isomers $4^-, 7^-$ in ^{252}No and $4^-, 6^-, 7^-$ in ^{254}No are also predicted. In ^{254}No , the $K^\pi = 3^+$ isomer should be accompanied by the nearby $K^\pi = 4^+$ counterpart. It is shown that, in the chain $^{250-262}\text{No}$, some features of ^{252}No and ^{254}No should exhibit essential irregularities caused by a noticeable shell gap in the neutron single-particle spectrum and corresponding reduction of the neutron pairing. In particular, low-energy pairing vibrational $K^\pi = 0^+$ states in $^{252,254}\text{No}$ are predicted.

I. INTRODUCTION

Spectroscopy of transfermium nuclei (Pu, Cm, Cf, Fm, No) is presently of a large interest, see reviews [1–3] and references therein. These nuclei provide valuable information on the single-particle spectra and pairing in heavy nuclei, which in turn can be useful for understanding the features of neighbouring superheavy nuclei. Though experimental spectroscopic information for transfermium nuclei is permanently increasing (see early [4–8] and recent [9–12] experimental studies), it still remains rather scarce. Among transfermium nuclei, nobelium isotopes have, perhaps, the most extensive experimental spectroscopic data [1, 2, 13].

In nobelium isotopes, ^{252}No and ^{254}No are most investigated [1, 2]. In these two nuclei, long ground-state rotational bands (up to $I^\pi = 20^+$ in ^{252}No and $I^\pi = 24^+$ in ^{254}No) are observed. Already for two decades, two-quasiparticle (2qp) $K^\pi = 8^-$ isomers (at 1.254 MeV in ^{252}No and 1.295 MeV in ^{254}No) are scrutinized by both experiment and theory. Some low-energy rotational bands with band heads $K^\pi = 2^-$ at 0.929 MeV in ^{252}No and $K^\pi = 3^+$ at 0.987 MeV in ^{254}No are found. Quite recently nonrotational states $K^\pi = 4^+$ (1.203 MeV) and 0^+ (0.888 MeV) in ^{254}No were tentatively observed [10]. The 0^+ state was treated as a result of the coupling between “normal” deformed and superdeformed shapes.

While the experimental information on nobelium isotopes is generally poor, there are already a lot of theoretical studies and predictions. The quadrupole moments and corresponding quadrupole deformations were estimated, see e.g. [14–19]. Single-particle (s-p) spectra, moments of inertia and pairing effects were systematically explored within the cranked relativistic Hartree-

Bogoliubov (CRHB) theory [17, 18]. The results from different density functional theories (DFT), including relativistic covariant [20], Skyrme [21] and Gogny [22], were critically compared [19]. Various multipole low-energy two-quasiparticle (2qp) excitations were considered in self-consistent calculations with Gogny force [16]. The investigation of s-p spectra, deformations, pairing and α -decay features in nobelium isotopes was recently performed within the symmetry-unrestricted nonrelativistic mean-field model employing a shell correction analysis [23].

Further, long rotational bands in $^{252,254}\text{No}$ were investigated within CRHB theory [17, 18, 24], cranked shell model [25–27], Skyrme-Hartree-Fock-Bogoliubov and Lipkin-Nogami (LN) methods [28], and interacting-boson model (IBM) [29].

The relation between the lowest 1^- states and reflection asymmetry in nobelium isotopes was studied [30]. Within the cluster model, the alternative parity bands based on the ground 0^+ and vibrational 1^- states were predicted as a consequence of the reflection asymmetry [31]. The scissor mode was measured [32] and analyzed within the Wigner Function Method [33].

K -isomers in $^{252,254}\text{No}$ were also widely explored, see e.g. [4–6, 10–12, 26, 27, 34–38]. Two-quasiparticle K -isomers $8^-, 2^-$ and 3^+ were considered in the framework of schematic QRPA approach [34, 35] using Woods-Saxon (WS) potential and pairing blocking at the Bardeen-Cooper-Schrieffer (BCS) level. In the two-quasiparticle approximation, the same isomers were analyzed with the universal WS potential and pairing treated within LN procedure [5, 6, 12]. In the studies [5, 6, 8, 12], the complete decay scheme for isomers 8^- was suggested (though being disputed in the recent experiment [10, 11]). Within

the cranking shell model (Nilsson potential with hexadecapole deformation) + pairing with the particle-number projection (CSM+PNP), a nice description of the energy of 8^- -isomer in ^{254}No was obtained [37]. Using the two-center shell model, α -decays relevant for the K -isomers were explored [36]. In recent shell model calculations [27], the energies of 8^- and 3^+ isomers in ^{254}No were well reproduced. Nevertheless, despite impressive theoretical progress, there are still some open problems. For example, the 2qp assignment of 8^- isomer in ^{254}No is still disputed [1, 2, 10–12].

A significant part of the previous theoretical studies was performed within non self-consistent models. However, even modern self-consistent models still produce rather different results and have troubles with the description of shell structures and other features observed in experiments, see discussion [1, 2, 19]. Moreover, most of the previous studies were devoted to description of the mean-field, pairing, rotation and decay properties. At the same time, the self-consistent predictions for low-energy non-rotational states still remain very limited.

In this connection, we present here a thorough investigation of non-rotational low-energy spectra in $^{250-262}\text{No}$ within fully self-consistent QRPA model [39–41] with Skyrme forces SLy4 [42], SLy6 [42], SkM* [43] and SVbas [44]. The main attention is paid to ^{252}No and ^{254}No , where we consider the observed K -isomers (as relevant test cases) and the lowest one-phonon states with $K^\pi = 0^+, 2^+, 3^+, 4^+, 0^-, 1^-, 2^-$ up to excitation energy 2–2.5 MeV. Note that at $N=152$ a shell gap in the neutron single-particle spectrum was predicted [6]. So one may expect in ^{254}No and nearby nuclei a significant reduction of the neutron pairing and subsequent irregularities in features. To test the pairing in these nuclei, we calculate the lowest pairing vibrational one-phonon $K^\pi = 0^+$ states which are a good indicator of the actual pairing.

It is important that the applied Skyrme forces have different isoscalar effective masses m^*/m affecting the distribution of single-particle states near the Fermi level [45]. Moreover, the applied Skyrme forces exploit different kinds of the pairing: volume in SLy4, SLy6 and SkM* and surface density-dependent in SVbas. The SLy4 and SLy6 belong to one family of Skyrme forces [42] and are rather similar. We use both them to demonstrate that in heavy nuclei even similar forces can lead to essentially different BCS description of the pairing.

Special attention is paid to isomers 8^- in $^{252,254}\text{No}$. Since in these isotopes the drop of the neutron pairing can take place, we additionally scrutinize this case with Skyrme functionals UNEDF1 [46], UNEDF2 [47] and UNEDF1^{SO} [28] employing LN procedure for the pairing.

The paper is organized as follows. In Sec. II, the model and details of the calculations are briefly described. In Sec. III, the trends and irregularities in features of $^{250-262}\text{No}$ are discussed. The single-particle spectra in $^{252,254}\text{No}$ are demonstrated. The pairing features and two-neutron mass staggering are considered as finger-

TABLE I. Isoscalar effective mass m^*/m , proton and neutron pairing constants G_p and G_n , kind of pairing (volume, surface) and IS and IV spin-orbit parameters b_4 and b'_4 for SLy4, SLy6, SkM* and SVbas. The surface pairing parameter is $\rho_{\text{pair}}=0.2011 \text{ fm}^{-3}$.

force	m^*/m	kind of pairing	G_p	G_n	b_4	b'_4
			(MeV fm ³)	(MeV fm ⁵)		
SLy4	0.70	volume	295.37	286.67	61.5	61.5
SLy6	0.69	volume	298.76	288.52	61.0	61.0
SkM*	0.79	volume	279.08	258.96	65.0	65.0
SVbas	0.90	surface	674.62	606.90	62.3	34.1

prints of shell gaps. In Sec. IV, various multipole low-energy 2qp and one-phonon QRPA states in $^{252,254}\text{No}$ are analyzed, K -isomers are thoroughly discussed, pairing vibrational states are demonstrated. In Sec. V, the conclusions are drawn. In Appendix A, the UNEDF1, UNEDF2 and UNEDF1^{SO} results for isomers in $^{252,254}\text{No}$ are presented.

II. MODEL AND CALCULATION DETAILS

The calculations are performed within QRPA model [39–41] based on Skyrme functional [21]. The model is fully self-consistent since i) both mean field and residual interaction are derived from the same Skyrme functional, ii) the contributions of all time-even densities and time-odd currents from the functional are taken into account, iii) both particle-hole and pairing-induced particle-particle channels are included, iv) the Coulomb (direct and exchange) parts are involved in both mean field and residual interaction.

A representative set of Skyrme parametrizations (SLy4 [42], SLy6 [42], SkM* [43] and SVbas [44]) with various isoscalar effective masses m^*/m and different kinds of the paring is used, see Table I. Besides, these forces have different isoscalar (IS) and isovector (IV) spin-orbit parameters. As mentioned above, SLy4 and SLy6 belong to the same family of Skyrme forces and are rather similar. As compared with the basic parametrization SLy4, the parameters of SLy6 were fitted with an additional two-body center-of-mass correction in the energy functional.

The method QRPA is implemented in a matrix form [39]. Spurious admixtures caused by violation of the translational and rotational invariance and by pairing-induced mixed particle number are removed using the technique of Ref. [41]. The states $K^\pi = 0^+, 2^+, 3^+, 4^+, 0^-, 1^-, 2^-, 3^-, 8^-$ are calculated as one-phonon excitations of multipolarity $\lambda\mu=20, 22, 43, 44, 30, 31, 32, 33, 98$, respectively.

The single-particle spectra and pairing characteristics are calculated with the code SKYAX [48] using two-dimensional (2D) grid in cylindrical coordinates. The grid step 0.7 fm and calculation box up to 3 nuclear radii

are employed. All proton and neutron s-p levels from the bottom of the potential well up to +40 MeV are taken into account. For example, SLy6 calculations for ^{254}No employ 1779 proton and 2035 neutron s-p levels.

The equilibrium axial quadrupole deformations

$$\beta = \frac{4\pi}{3} \frac{Q_2}{AR^2} \quad (1)$$

and the related intrinsic quadrupole moments

$$Q_2 = \sum_{q=p,n} \int d^3r (2z^2 - x^2 - y^2) \rho_q(\mathbf{r}) \quad (2)$$

are obtained at the minimum of the total nuclear energy. Here, A is the mass number, $R=r_0 A^{1/3}$ with $r_0 = 1.2$ fm is the nuclear radius and $\rho_q(\mathbf{r})$ are proton ($q = p$) and neutron ($q = n$) densities in the ground state (g.s.).

For the pairing, the zero-range pairing interaction [49]

$$V_q^{\text{pair}}(\mathbf{r}, \mathbf{r}') = -G_q \left[1 - \eta \left(\frac{\rho(\mathbf{r})}{\rho_{\text{pair}}} \right) \right] \delta(\mathbf{r} - \mathbf{r}'), \quad (3)$$

is used, where G_q are proton and neutron pairing strength constants (shown in Table I). The pairing is treated within the BCS scheme [40]. The strength constants are fitted to reproduce empirical pairing gaps in selected isotopic and isotonic chains [50]. To cope with a divergent character of zero-range pairing forces, the energy-dependent cut-off is used [40, 49]. The volume density-independent and surface density-dependent cases of pairing are realized at $\eta=0$ and 1, respectively. The model parameter ρ_{pair} is 0.2011 fm^{-3} is determined in the SVbas fit [44].

The pairing (3) results in state-dependent pairing gaps $\Delta_q(i)$ [44, 49]. Then it is convenient to evaluate the pairing by *average* spectral pairing gaps

$$\Delta_q = \frac{\sum_{i \in q} v_i u_i \Delta_q(i)}{\sum_{i \in q} v_i u_i} \quad (4)$$

where v_i and u_i are Bogoliubov pairing factors for quasi-particle states i . These spectral gaps usually well correspond to the five-point experimental gaps $\Delta_q^{(5)}$ in mid-shell regions [49].

The calculations use a large 2qp configuration space. The energy weighted sum rules (EWSR) for $\lambda=0,1,2,3$ are exhausted by 90-100%.

The moments of inertia (MoI) are calculated using the Thouless-Valatin expression [51]

$$J = 2 \sum_{\nu} \frac{|\langle \nu | I_x | 0 \rangle|^2}{E_{\nu}} \quad (5)$$

where I_x is x-component of the operator of the total angular moment I , $|0\rangle$ is the QRPA vacuum and $|\nu\rangle$ is the excited QRPA state with the energy E_{ν} . For rotational energies, we use formula [52]

$$E_I = \frac{I(I+1)}{2J}. \quad (6)$$

The reduced probabilities ($\lambda > 1$)

$$B(E\lambda\mu) = e^2 (2 - \delta_{\mu,0}) |\langle \nu | F(E\lambda\mu) | 0 \rangle|^2 \quad (7)$$

for $E\lambda\mu$ -transitions from the ground state $|0\rangle$ with $I^{\pi}K = 0^+0_{\text{gs}}$ to the QRPA state $|\nu\rangle$ with $I^{\pi}K$ ($I = \lambda, K = \mu, \pi = (-1)^{\lambda}$) are computed with the transition operator

$$F(E\lambda\mu) = \sum_{i=1}^Z [r^{\lambda} Y_{\lambda\mu}(\Omega)]_i. \quad (8)$$

The transition probabilities are estimated in Weisskopf units $W.u. = [3R^{\lambda}/(\lambda + 3)]^2/(4\pi) e^2 \text{ fm}^{2\lambda}$.

The normalized $E0$ transition probability for the decay $0^+0_{\nu} \rightarrow 0^+0_{\text{gs}}$ is described by the dimensionless value

$$\rho^2(E0) = \frac{1}{R^4} |\langle 0 | F(E0) | \nu \rangle|^2 \text{ with } F(E0) = \sum_{i=1}^Z r_i^2. \quad (9)$$

TABLE II. The calculated and experimental [13] quadrupole deformations β , moments of inertia J , proton Δ_p and neutron Δ_n pairing spectral average gaps, energies $E(2_1^+)$ of the lowest rotational $I^{\pi} = 2^+$ states in $^{252,254}\text{No}$.

Nucleus		SLy4	SLy6	SkM*	SVbas	exp
^{252}No	β	0.303	0.300	0.306	0.299	
	$J (\hbar^2/\text{MeV})$	79.9	76.8	74.1	58.0	64.7
	Δ_p (MeV)	0.48	0.52	0.38	0.56	0.67
	Δ_n (MeV)	0.32	0.33	0.51	0.70	0.71
	$E(2_1^+)$ (keV)	38	39	40	52	46
^{254}No	β	0.304	0.298	0.304	0.298	
	$J (\hbar^2/\text{MeV})$	76.0	78.3	80.8	59.3	67.9
	Δ_p (MeV)	0.47	0.52	0.40	0.55	0.66
	Δ_n (MeV)	0.28	0.05	0.36	0.67	0.71
	$E(2_1^+)$ (keV)	39	38	37	50	44

III. MEAN-FIELD AND PAIRING FEATURES OF NOBELIUM ISOTOPES

Some calculated and experimental characteristics of $^{252,254}\text{No}$ are shown in Table II. The experimental pairing gaps Δ_q are obtained by five-point pairing formula using evaluations for binding energies [53]. The experimental MoI are evaluated as $J = 3/E(2_1^+)$ where $E(2_1^+)$ is the measured energy of $I^{\pi} = 2^+$ state of the g.s. rotational band.

Following Table II, the applied forces provide a rough description of the experimental $E(2_1^+)$ -energies and MoI. To the best of our knowledge, there is no experimental data for quadrupole deformations β in $^{252,254}\text{No}$. However, all the forces give similar results for β , which are in a good agreement with the values of macroscopic-microscopic model [14], see the comparison in Ref. [15].

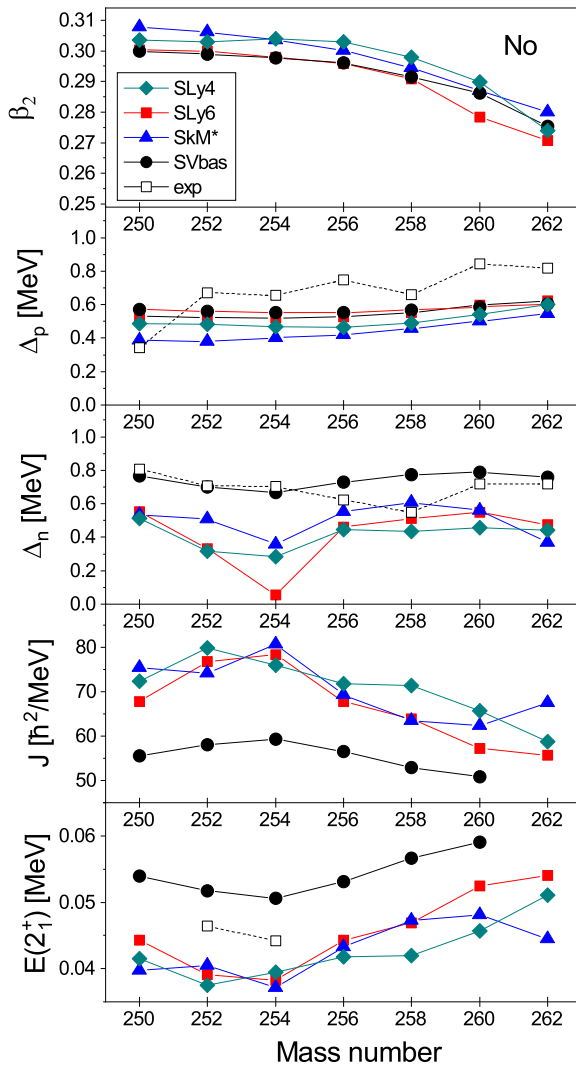


FIG. 1. Deformations β , moments of inertia J , spectral average pairing gaps $\Delta_{n,p}$, and energies $E(2_1^+)$ in $^{250-262}\text{No}$, calculated with the forces SLy4 (green diamonds), SLy6 (red filled squares), SkM* (blue filled triangles) and SVbas (black filled circles). The experimental values for pairing gaps and energies $E(2_1^+)$ [13] are shown by open squares.

Note that, following the study [54], the quadrupole triaxial and octupole deformations in $^{252,254}\text{No}$ near the main minimum of potential energy surface (PES) at $\beta \approx 0.3$ are negligible.

Table II shows that SVbas provides the most reasonable description of the experimental pairing gaps $\Delta_{p,n}$. In particular, SVbas gives $\Delta_n > \Delta_p$ in accordance with the experiment. Instead, SLy4, SLy6 and SkM* demonstrate a weaker neutron pairing and even its collapse in ^{254}No for SLy6. The latter is caused by using BCS technique in the case of a weak pairing. Following our analysis, the similar forces SLy4 and SLy6 give essentially different BCS results for neutron pairing in ^{254}No because for SLy4 the density of neutron s-p states near the Fermi

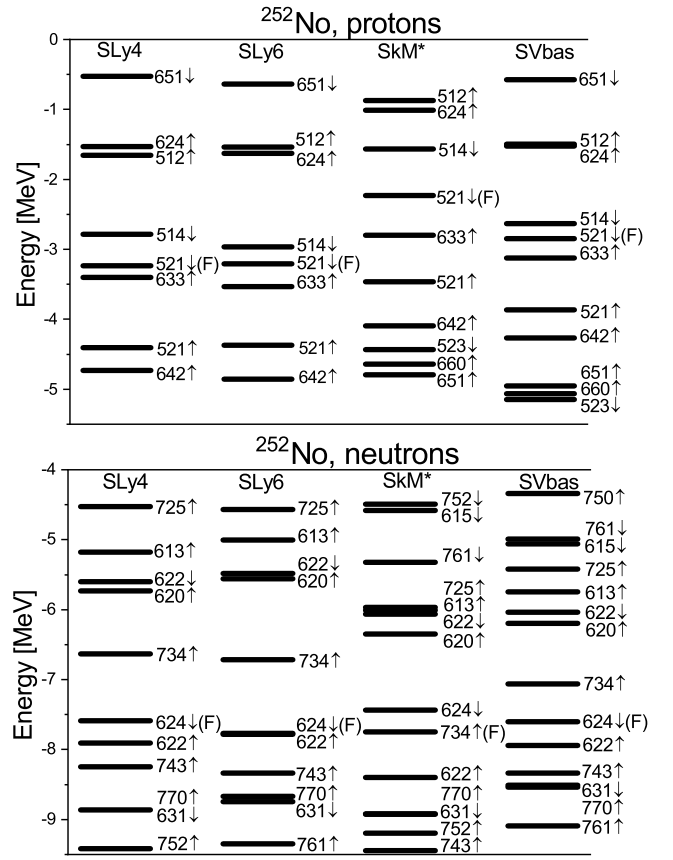


FIG. 2. SLy4, SLy6, SkM* and SVbas proton and neutron s-p spectra near the Fermi levels (F) for ^{252}No .

level in this nucleus is slightly larger than for SLy6 (see Fig. 3 for the comparison). This demonstrates how fragile could be the calculation results in heavy nuclei.

The collapse of the neutron pairing for SLy6 in ^{254}No is seen in Fig. 1, where various characteristics of nobelium isotopes are displayed. SLy4, SkM* and SVbas also give some minima in Δ_n for ^{254}No but these minima are much softer, especially for SVbas. Note that a similar distinctive minimum in Δ_n was also obtained at $N=149-151$ using Skyrme, Gogny and covariant relativistic density energy functionals [19]. Following Fig. 1, just the drop of the neutron pairing causes the irregularity in A -dependence of MoI and $E(2_1^+)$. Instead, the deformation β in nobelium isotopes changes smoothly and can lead only to a gradual change of these values.

Fig. 1 also shows experimental $\Delta_{n,p}$ evaluated by five-point formula with the nuclear binding energies from Ref. [53]. This formula is commonly used to get smooth pairing gaps among the neighboring nuclei, see discussion [49]. It is seen that we rather well describe proton pairing gaps Δ_p but not neutron gaps Δ_n . Unlike our results, the experimental Δ_n exhibit a minimum at $A=252$ and a plateau at $A=252-254$.

To understand the origin of Δ_n -minimum in our calculations, let's consider SLy4, SLy6, SkM* and SVbas

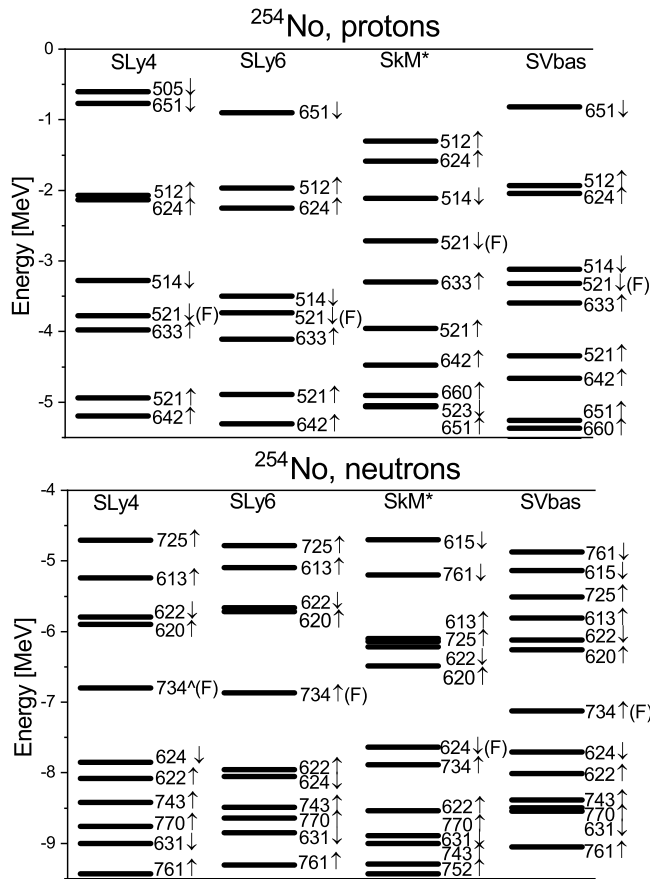


FIG. 3. The same as in Fig. 2 but for ^{254}No .

s-p proton and neutron spectra in $^{252,254}\text{No}$, exhibited in Figs. 2 and 3. The s-p levels in the figures are marked by Nilsson asymptotic numbers $[N, n_z, \Lambda]$, where N is the principle quantum number, n_z is the fraction of N along z-axis and Λ is projection of the orbital moment onto z-axis [55].

Figure 2 for ^{252}No shows that, for all four Skyrme forces, the proton Fermi level lies in rather dense spectrum and so we have a significant proton pairing. Instead, in the neutron case, SLy4 and SLy6 Fermi level $[624 \downarrow]$ lies at the boundary of a wide shell gap, which leads to a small $\Delta_n = 0.32\text{--}0.33$ MeV. Actually, this particular neutron spectral configuration is not a true shell gap since it separated by the orbital $[734 \uparrow]$ into two parts. It is rather a region of a low level density. Nonetheless, for simplicity the term "shell gap" is used hereafter.

In Fig. 3 for ^{254}No , the SkM* neutron Fermi level lies near the shell gap and so we have a significant minimum in Δ_n depicted for this force in Fig. 1. For SLy4 and SLy6, the neutron Fermi level $[734 \uparrow]$ enters the center of the shell gap, which results in a small $\Delta_n = 0.28$ MeV for SLy4 and collapse of the neutron pairing for SLy6. The difference in SLy4 and SLy6 results is caused by a different energy gap between Fermi (F) and next (F+1) levels, which is 0.90 MeV in SLy4 and 1.15 MeV in SLy6.

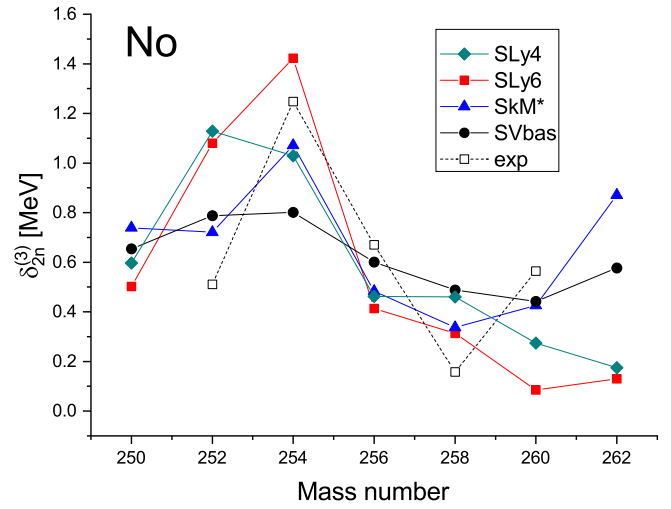


FIG. 4. SLy4, SLy6, SkM*, SVbas and experimental neutron values $\delta_{2n}^{(3)}$ in nobelium isotopes.

The smaller gap for SLy4 prevents the BCS collapse of the neutron pairing. Our SLy4 and SLy6 results for the shell gap in neutron s-p spectrum in ^{254}No agree well with the previous calculations using the Woods-Saxon mean field [6] and various self-consistent s-p potentials (Skyrme SLy4 and UNEDF2, Gogny DS1 and DM1 and relativistic NL3*) [19]. These calculations also give at $\beta \approx 0.3$ a significant neutron shell gap with the Fermi level $[734 \uparrow]$ in the middle of the gap. Besides, a gap at $N=152$ was demonstrated in cranked-shell-model calculations [38]. In Figs. 2 and 3, SVbas gives the same neutron Fermi levels as SLy4 and SLy6. Instead, in SkM*, the neutron levels $[734 \uparrow]$ and $[624 \downarrow]$ are swapped and so SkM* suggests other neutron Fermi levels in $^{252,254}\text{No}$.

A considerable shell gap in the neutron s-p spectra should affect features of several isotopes (from ^{250}No to ^{258}No) since their Fermi levels lie either near ($[624 \downarrow]$, $[622 \uparrow]$, $[620 \uparrow]$, $[622 \downarrow]$ or inside the gap ($[734 \uparrow]$). In particular, one may expect a suppression of Δ_n in these four isotopes. Then the difference in the minima of calculated and experimental Δ_n , exhibited in Fig. 1, is not surprising. Note also that, in the case of shell gaps, values Δ_q manifest rather mean-field effects than the paring impact (see a general discussion [49]).

To clarify more the point with the neutron shell gap, it is worth to consider the neutron mass staggering quantity

$$\begin{aligned} \delta_{2n}^{(3)}(N, Z) &= S_{2n}(N, Z) - S_{2n}(N + 2, Z) \\ &= 2B(N, Z) - B(N - 2, Z) - B(N + 2, Z), \end{aligned} \quad (10)$$

which is typically used to identify two-neutron shell gaps, see e.g. [19, 23]. Here, $S_{2n}(N, Z)$ is the two-neutron separation energy and $B(N, Z)$ is the nuclear binding energy. In Fig. 4, the calculated $\delta_{2n}^{(3)}$ are compared with experimental ones evaluated using the experimental binding energies [13, 53]. It is seen that, in accordance with our SLy6, SkM* and SVbas calculations, the experimental

TABLE III. Experimental [13] and calculated ground and first excited non-rotational I^π states in Z -odd and N -odd neighbours of ^{252}No and ^{254}No . The experimental assignments in the parentheses are tentative.

Nucl.	exp	SLy4	SLy6	SkM*	SVbas
^{252}No					
^{251}No	$(7/2^+), (1/2^+)$	$7/2^+, 5/2^+$	$7/2^+, 5/2^+$	$9/2^-, 7/2^+$	$7/2^+, 5/2^+$
^{253}No	$(9/2^-), 5/2^+$	$9/2^-, 1/2^+$	$9/2^-, 7/2^+$	$7/2^+, 9/2^-$	$9/2^-, 7/2^+$
^{251}Md	$7/2^-, 1/2^-$	$1/2^-, 7/2^+$	$1/2^-, 7/2^-$	$1/2^-, 7/2^-$	$1/2^-, 7/2^-$
^{253}Lr	$(7/2^-), (1/2^-)$	$7/2^-, 1/2^-$	$7/2^-, 1/2^-$	$7/2^-, 9/2^+$	$7/2^-, 1/2^-$
^{254}No					
^{253}No	$(9/2^-), 5/2^+$	$9/2^-, 1/2^+$	$9/2^-, 5/2^+$	$7/2^+, 9/2^-$	$9/2^-, 7/2^+$
^{255}No	$(1/2^+)$	$1/2^+, 3/2^+$	$1/2^+, 3/2^+$	$1/2^+, 3/2^+$	$1/2^+, 3/2^+$
^{253}Md	$(7/2^-)$	$1/2^-, 7/2^+$	$1/2^-, 7/2^-$	$1/2^-, 7/2^+$	$1/2^-, 7/2^-$
^{255}Lr	$(1/2^-), (7/2^-)$	$7/2^-, 1/2^-$	$7/2^-, 1/2^-$	$7/2^-, 9/2^+$	$7/2^-, 1/2^-$

$\delta_{2n}^{(3)}$ also exhibits a peak at $A=254$. For SLy4, the value $\delta_{2n}^{(3)}$ grows at $A=252$ -254 with a maximum at $A=252$, which contradicts the experimental data. Altogether, Fig.4 justifies the existence of the neutron shell gap and its maximal impact for ^{254}No .

A similar result for $\delta_{2n}^{(3)}$ was obtained in calculations [19, 23]. In Ref. [23], the computed pairing gap Δ_n has no a distinctive minimum at $N=152$. Perhaps, this is caused by using the LN prescription which prevents the pairing breakdown. However, the LN procedure does not yet ensure a proper description of the paring in trans-fermium nuclei. For example, in CRHB studies [17, 18] an additional manual attenuation of the paring strength by 10-12% was used to get a proper description of the moments of inertia.

A quality of the calculated s-p spectra in $^{252,254}\text{No}$ can be additionally checked by identification of ground and first excited states on the neighboring N -odd and Z -odd nuclei. In Table III, we compare our results for odd nuclei with the experimental data [13]. Note that in many cases (marked by parenthesis in the table) we deal with a tentative experimental assignment of the states. In our estimation, the first excited state is determined as the closest to the Fermi level in the s-p spectrum of the odd nucleus. The states in the upper and bottom parts of the table are determined separately from s-p spectra of ^{252}No and ^{254}No , exhibited in Figs. 2 and 3.

Table III shows that SLy6 demonstrates the best performance. It correctly indicates the ground states in all N -odd nuclei and in ^{253}Lr . In other Z -odd nuclei, this force permutes the ground and first excited states. The SLy4 and SVbas descriptions are somewhat worse. The performance of SkM* is unsatisfactory. This force reproduces the ground states only in ^{255}No and ^{253}Lr . So, SLy6 and SVbas s-p spectra near the Fermi level are most robust. The description of the neutron spectra is better than of proton ones.

IV. LOW-ENERGY SPECTRA IN $^{252,254}\text{NO}$

In this section, we analyze low-energy ($E_\nu < 2.5$ MeV) states with $K^\pi = 0^+, 2^+, 3^+, 4^+, 0^-, 1^-, 2^-, 3^-, 8^-$ in $^{252,254}\text{No}$. Since the forces SLy4 and SLy6 are rather similar, we provide SLy4 results only for the states with available experimental data: $K^\pi = 0^+, 3^+, 4^+, 2^-, 8^-$.

A. Isomers $K^\pi = 8^-$

As a first step, we consider two-quasiparticle 8^- isomers in ^{252}No and ^{254}No , discussed in reviews [1, 2]. The appearance of these isomers is explained by occurrence in these nuclei of high- K s-p states near the Fermi level. Excitation energies of 8^- isomers should be sensitive to the s-p spectra and pairing. Thus these isomers are the robust test of the model. In our calculations, $K^\pi = 8^-$ isomers are QRPA states of electric multipolarity $\lambda\mu=98$, where $K = \mu$ and $\pi = (-1)^\lambda$.

The 8^- state at 1.254 MeV in ^{252}No is usually assigned as neutron 2qp configuration $nn[624 \downarrow, 734 \uparrow]$ [1, 2, 38, 56]. The same assignment is obtained in our QRPA calculations for all four applied Skyrme forces, see Table IV. Our calculations predict this isomer as $F \rightarrow F + 1$ excitation where F is the Fermi level and $F + 1$ is the next one.

Following Table IV, SLy4 very well describes the experimental $E_x=1.254$ MeV of 8^- state in ^{252}No . The forces SLy6 and SkM* slightly overestimate the experimental values. A much larger overestimation takes place for SVbas where the pairing is the most developed. In the case of the developed pairing, the pairing blocking can decrease the calculated energies of 2qp states by 0.2-0.5 MeV [35, 45]. However, the calculations with the particle-number projection for rare-earth nuclei [57] show that the blocking effect too strongly suppresses the pairing in 2qp states.

Table IV shows that QRPA 8^- state in ^{252}No is basically formed by one 2qp component. At the same time, the impact of residual interaction is also noticeable. In-

TABLE IV. Characteristics of the lowest ($\nu=1$) calculated 8^- states in $^{252,254}\text{No}$: QRPA excitation energies E_ν , reduced transition probabilities $B(E98)$, main 2qp components qq' , their energies $\epsilon_{qq'}$, contributions to the state norm $N_{qq'}$ and F-order. For the convenience of the discussion, for ^{254}No the second ($\nu=2$) 8^- states are also depicted.

Force	E (MeV)	$B(E98)$ (W.u.)	qq'	$\epsilon_{qq'}$ (MeV)	$N_{qq'}$	F-order
$^{252}\text{No}, E_x=1.254$ MeV						
SLy4	1.257	0.022	$nn[624 \downarrow, 734 \uparrow]$	1.211	0.998	F,F+1
SLy6	1.361	0.038	$nn[624 \downarrow, 734 \uparrow]$	1.317	0.996	F,F+1
SkM*	1.330	0.025	$nn[734 \uparrow, 624 \downarrow]$	1.198	0.992	F,F+1
SVbas	1.913	0.119	$nn[624 \downarrow, 734 \uparrow]$	1.751	0.912	F,F+1
$^{254}\text{No}, E_x=1.295$ MeV						
SLy4	1.673	0.009	$nn[734 \uparrow, 613 \uparrow]$	1.695	0.996	F,F+3
	1.996	0.444	$pp[514 \downarrow, 624 \uparrow]$	1.994	0.847	F+1, F+2
SLy6	1.747	0.014	$nn[734 \uparrow, 613 \uparrow]$	1.780	0.994	F,F+3
	2.040	0.578	$pp[514 \downarrow, 624 \uparrow]$	1.966	0.993	F+1, F+2
SkM*	1.554	0.333	$pp[514 \downarrow, 624 \uparrow]$	1.482	0.990	F+1,F+2
	1.645	0.0003	$nn[734 \uparrow, 624 \downarrow]$	1.610	0.985	F-1,F
SVbas	1.994	0.370	$pp[514 \downarrow, 624 \uparrow]$	1.751	0.791	F+1,F+2
	2.034	0.049	$nn[734 \uparrow, 613 \uparrow]$	2.026	0.811	F,F+3

deed, the collective shift $\Delta E_{\text{coll}} = E_{\nu=1} - \epsilon_{qq'}$ is 46, 44, 132 and 162 keV for SLy4, SLy6, SkM* and SVbas, respectively. The residual interaction upshifts the energy of the lowest 8^- state as compared with minimal $\epsilon_{qq'}$. This means that IV residual interaction overrides IS one.

The reduced transition probabilities $B(E98)$ for 8^- states with one dominant neutron 2qp pair are obviously small since the electric transition operator (8) includes only the proton part. Instead, 8^- states with a large proton contribution are characterized by significant $B(E98)$ values. In ^{254}No , the direct decay of 8^- isomer to 8^+ member of the ground state band was observed [8, 12]. However, this decay was not caused by an external electric field and so cannot be considered as a justification of the proton structure of the 8^- isomer. The deexcitation of the neutron 8^- isomer can also occur through a measurable γ -decay.

Following Table IV, the description of 8^- state in ^{254}No is much worse than in ^{252}No . The energy of this state is significantly overestimated by all four Skyrme forces. Moreover, these forces predict three different 2qp configurations for 8^- state. The neutron assignment from SLy4 and SLy6 looks more relevant since it treats 8^- excitation as 1ph transition $F \rightarrow F+3$. Instead, SkM* and SVbas suggest the proton particle-particle transition $F+1 \rightarrow F+2$, which can occur only at the condition of well developed proton pairing. Note that our calculations for ^{254}No predict a suppression of the neutron pairing but not of the proton one. Note also that the neutron 1ph transition $624 \downarrow \rightarrow 734 \uparrow$, which gives 8^- state in ^{252}No , becomes particle-particle in ^{254}No and so is suppressed.

For the lowest 8^- state in ^{254}No , we again see a noticeable impact of the residual interaction. However now the collective shifts have different signs displaying a dominance of IS interaction for SLy4 and SLy6 and of IV interaction for SkM* and SVbas.

The 8^- isomer in ^{254}No was earlier investigated within various models, see e.g. [26, 34–37]. The models [34, 35] use Woods-Saxon single-particle potential and schematic residual interaction, i.e. these models are not self-consistent. At the same time, they implement the pairing blocking which allows to get a reasonable description of the energy of lowest 2qp 8^- state in ^{254}No (1.4 MeV [34] and 1.3 MeV [35]). These models suggest different assignments for the state: $nn[734 \uparrow, 613 \uparrow]$ in Ref. [34] and $pp[514 \downarrow, 624 \uparrow]$ in Ref. [35]. These assignments correlate with our results in Table IV. The Nilsson cranking model with the pairing projection [37] predicts the assignment $pp[514 \downarrow, 624 \uparrow]$ and suggests the state energy 1.272 MeV in a good agreement with the experimental value. Altogether, studies [26, 34, 35, 37] show that the pairing blocking and projection are important for reproduction of E_x . In particular, this is confirmed by a good description of the energy of 8^- state by shell model with projection-after-variation prescription [26].

Following previous [34, 35] and our calculations, the different 2qp assignments of 8^- isomer can be explained by close excitation energies of 2qp states $nn[734 \uparrow, 613 \uparrow]$ and $pp[514 \downarrow, 624 \uparrow]$ in ^{254}No . So, even a modest difference in the s-p spectra can result in different assignments. Anyway, all the models predict that 8^- state in ^{254}No is dominated by one 2qp configuration. The calculations [34] show that, for this state, the coupling with complex configurations is negligible. The two-center shell model [36] gives the proton 2qp 8^- state at ≈ 1.27 MeV but here a good description of the energy is obtained by a manual decrease of the pairing strength by 15%.

A more accurate 2qp assignment of the 8^- state in ^{254}No could be done using experimentally observed γ -decays to and from this state. However, even here we have different conclusions. While the exploration [7] suggests the proton configuration $pp[514 \downarrow, 624 \uparrow]$, the

study [8] favors one of two neutron configurations, $nn[734 \uparrow, 613 \uparrow]$ and $nn[734 \uparrow, 624 \downarrow]$. The neutron assignments [8] look more reasonable since they are argued by the measured γ -decay from the neutron two-quasiparticle isomer $K^\pi = 10^+$ $nn[734 \uparrow, 725 \uparrow]$ located at 2.01 MeV to the rotational band built on the $K^\pi = 8^-$ state. Indeed, at the neutron assignments, the γ -decay involves the transition of a single neutron. Following our SLy6 calculations, this could be 0.5-MeV transition $725 \uparrow (F+4) \rightarrow 613 \uparrow (F+3)$ or 3.4-MeV transition $725 \uparrow (F+4) \rightarrow 624 \uparrow (F-2)$. The former looks more realistic since its transition energy is closer to the experimental energy difference $E_{10^+} - E_{8^-} = 2.012 - 1.295 = 0.717$ MeV. So, the decay analysis [8] confirms our SLy6 assignment $nn[734 \uparrow, 613 \uparrow]$ shown in Table. IV. Note also that, in a good agreement with results [8], our SLy6 calculations give the lowest 2qp neutron $K^\pi = 10^+$ $nn[734 \uparrow, 725 \uparrow]$ state at 1.93 MeV, i.e. close to the experimental value 2.01 MeV.

The scenario [8] was recently questioned by measurements [10, 11], where 2.01-MeV $K^\pi = 10^+$ band-head was replaced by $K^\pi = 11^-$ band-head with the corresponding change of the parity of the members of the rotational band. Following our QRPA calculations, the lowest non-rotational state $K^\pi = 11^-$ lies at 3.83 (SLy6), 4.04 (SkM*) and 3.51 (SVbas) MeV, i.e. much higher of the experimental energy 2.01 MeV. So, our calculations rather support the decay scheme [8].

The issue has become even more intriguing after publication of a new high-resolution γ -decay data for ^{254}No [12], which confirm and additionally specify the previous decay scheme [8]. However, unlike the previous study [8], the proton assignment $pp[514 \downarrow, 624 \uparrow]$ was suggested for 8^- isomer. This assignment was based on the calculation results ("universal" WS potential + LN procedure for the pairing) with the lowest proton 2qp configuration. Besides, this configuration was justified by decay of 8^- isomer to the rotational band of proton isomer $K^\pi = 3^+$. Actually, both neutron [8] and proton [12] assignments were justified by similar arguments but using different parts of the decay chain, the decay $10^+ \rightarrow 8^-$ in the analysis [8] and decay $8^- \rightarrow 3^+$ in the discussion [12]. We incline to arguments [8] since then we deal with $\Delta K = 2$ transition which should be much stronger than $\Delta K = 5$ one. Our SLy4 and SLy6 results for 8^- -isomer just confirm the neutron assignment $nn[734 \uparrow, 613 \uparrow]$.

As seen from Table IV, the energy interval between the lowest neutron and proton 2qp 8^- configurations in ^{254}No can be rather small, e.g. 186 keV for SLy6 and 128 keV for SkM*. These values are comparable with collective shifts mentioned above. So, in principle, one cannot exclude the mixture of the neutron and proton 8^- 2qp pairs by the residual $\lambda\mu=98$ interaction. This could partly reconcile two optional assignments [8] and [12] for 8^- isomer in ^{254}No .

To our opinion, just well established isomers 8^- and 2^- in ^{252}No and 3^+ in ^{254}No have to be used for the

primary testing of the theory. Moreover, only a simultaneous description of these isomers can justify the theory validity. To our knowledge, there was no yet theoretical studies which successfully describe this set of isomer's data. As for the disputed 8^- isomer in ^{254}No , its description demands very fine tuning of the s-p scheme and pairing and so it is worth to use this isomer only for the secondary fine tuning. In Appendix A we show that alternative Skyrme parametrizations (UNEDF1 [46], UNEDF1^{SO} [28] and UNEDF2 [47]) do not provide the simultaneous description of the isomers and, in this sense, demonstrate a worse performance than SLy6.

The above analysis as well as a good SLy6 description of 3^+ and 8^- in ^{252}No and 2^- state in ^{254}No (see below) show that this force is reasonable enough for the thorough inspection of the low-energy spectra in $^{252,254}\text{No}$. The force SLy4 supplements SLy6 by correcting its results in the case of a weak neutron pairing in ^{254}No .

B. Pairing vibrations $K^\pi = 0^+$

As mentioned above, our calculations predict a reduction of the neutron pairing in ^{254}No . This should lead to a significant downshift of the energy of $K^\pi = 0^+$ pairing vibrational states with a dominant neutron structure. Table V shows that this is indeed the case for SLy4, SLy6 and SkM* where the neutron pairing is suppressed. These forces give first 0_1^+ states below 1 MeV. The lowest energy 0.224 MeV is obtained for SLy6 where we have a collapse of the neutron pairing. Obviously, so low energy is an artifact of the BCS description of a weak pairing. In this connection, SLy4 energy 0.611 MeV for 0_1^+ state is more realistic (here we have a drop but not collapse of the neutron pairing). In ^{252}No , the forces SLy4, SLy6 and SkM* also give 0_1^+ -energies below 1 MeV. In both ^{252}No and ^{254}No , the 0_1^+ states are collective (the largest 2qp component exhausts only 33-58% of the state norm) and dominated by neutron contributions. The dominant neutron structure leads to small values of $B(E2)$ and $\rho^2(E0)$. In ^{254}No , the forces SLy4, SLy6 and especially SkM* also provide second 0_2^+ low-energy states.

For the forces with more developed neutron pairing, we get 0_1^+ states with basically proton structure (SkM* for ^{252}No and SVbas for $^{252,254}\text{No}$). The states are also collective but, because of the proton structure, exhibit large $B(E2)$ and $\rho^2(E0)$ values.

The $\rho^2(E0)$ values for $^{252,254}\text{No}$ in Table V are smaller than those in ^{282}Cn where they reach $\approx 21 \cdot 10^{-3}$ [58]. At the same time, our $\rho^2(E0)$ values correspond to QPM estimations for rare-earth and actinide nuclei [59, 60, 62].

The 0^+ states in Table V are mainly composed of *diagonal* 2qp configurations, which means that they are *pairing vibrations*. Such states are well known in even-even deformed nuclei in rare-earth [59–63] and actinide [62] regions. The most thorough analysis for low-energy 0^+ states was performed within QPM [60]. The lowest excited 0^+ states usually have the energy around 1 MeV.

TABLE V. Features of the lowest excited QRPA 0^+ states in $^{252,254}\text{No}$: QRPA excitation energies E , reduced transition probabilities $B(E20)$ and $\rho^2(E0)$, main two 2qp components qq' , their energies $\epsilon_{qq'}$, contributions to the state norm $N_{qq'}$ and F-order. For the sake of discussion, in ^{254}No , two lowest 0^+ states are exhibited.

Force	E (MeV)	$B(E20)$ (W.u.)	$\rho^2(E0)$ (10^{-3})	qq'	$\epsilon_{qq'}$ (MeV)	$N_{qq'}$	F-order
^{252}No							
SLy4	0.740	0.18	0.08	$nn[734 \uparrow, 734 \uparrow]$ $nn[624 \downarrow, 624 \downarrow]$	1.074 1.348	0.53 0.30	F+1, F+1 F,F
SLy6	0.774	0.02	0.29	$nn[734 \uparrow, 734 \uparrow]$ $nn[624 \downarrow, 624 \downarrow]$	1.070 1.563	0.58 0.17	F+1, F+1 F,F
SkM*	0.838	1.12	1.24	$pp[521 \downarrow, 521 \downarrow]$ $pp[514 \downarrow, 514 \downarrow]$	1.014 1.093	0.46 0.42	F,F F+1,F+1
SVbas	1.249	6.41	2.50	$pp[514 \downarrow, 514 \downarrow]$ $pp[521 \downarrow, 521 \downarrow]$	1.215 1.186	0.56 0.36	F+1,F+1 F,F
^{254}No							
SLy4	0.616	0.08	0.08	$nn[734 \uparrow, 734 \uparrow]$ $nn[620 \uparrow, 620 \uparrow]$	1.021 1.156	0.51 0.25	F, F F+1,F+1
	1.000	2.69	2.69	$pp[514 \downarrow, 514 \downarrow]$ $pp[521 \downarrow, 521 \downarrow]$	1.092 1.163	0.57 0.30	F+1,F+1 F,F
SLy6	0.224	0.002	0.01	$nn[734 \uparrow, 734 \uparrow]$ $nn[620 \uparrow, 620 \uparrow]$	1.048 1.267	0.41 0.27	F, F F+1,F+1
	1.133	1.32	1.98	$pp[514 \downarrow, 514 \downarrow]$ $pp[521 \downarrow, 521 \downarrow]$	1.155 1.152	0.56 0.45	F+1,F+1 F,F
SkM*	0.767	0.17	0.74	$nn[624 \downarrow, 624 \downarrow]$ $nn[620 \uparrow, 620 \uparrow]$	1.409 1.362	0.33 0.23	F,F F+1, F+1
	0.866	4.38	6.78	$pp[521 \downarrow, 521 \downarrow]$ $pp[514 \downarrow, 514 \downarrow]$	1.02 1.08	0.45 0.43	F,F F+1,F+1
SVbas	1.236	6.36	2.54	$pp[514 \downarrow, 514 \downarrow]$ $pp[521 \downarrow, 521 \downarrow]$	1.083 1.017	0.43 0.38	F+1,F+1 F,F
	1.454	0.53	1.35	$pp[633 \uparrow, 633 \uparrow]$ $pp[521 \downarrow, 521 \downarrow]$	1.593 1.186	0.45 0.25	F-1,F-1 F,F

Their reduced transition probabilities $B(E20, 0^+0_{\text{gs}} \rightarrow 2^+0)$ depend on the pairing strength and contribution of β -vibrations. Pairing vibrational states can be observed in (p, t) and (t, p) transfer reactions [59, 60]. Following QPM studies, the lowest $K_{\nu}^{\pi} = 0_1^+$ state usually has negligible two-phonon admixtures and so can be reasonably described within QRPA. One should distinguish pairing vibrational states from the low-lying 0^+ states arising from a shape coexistence [16, 64]. The description of the latters is beyond the scope of QPM and present QRPA method.

In the recent experiment for ^{254}No [10], an excited 0^+ state at 0.888 MeV was identified. For the moment, this is the lowest observed non-rotational state in the multipole spectrum of ^{254}No . Our SLy4 and SkM* results in Table V reasonably reproduce the energy of this state (for SkM* both first and second 0^+ states can pretend to describe the experiment). Following the theoretical predictions [16, 64], the authors of Ref. [10] treat the observed 0^+ state as a consequence of the coexistence of normally deformed and superdeformed shapes. The impact of the prolate and triaxial shapes is also admitted.

Our SLy4, SLy6, SkM* and SVbas calculations also predict for ^{254}No two deep minima in PES: the main minimum at "normal" deformation $\beta \approx 0.3$ and the second minimum at superdeformation $\beta \approx 0.9$ -1.0. However, our SkM* and SVbas calculations performed with $\beta \approx 0.3$ rather well reproduce the experimental energies of low-spin states of the g.s. rotational band in ^{254}No or somewhat underestimate them (SLy4, SLy6), see e.g. Figs. 5 and 6 below. Instead, if we use the superdeformation $\beta \approx 0.9$ -1.0, the moments of inertia become much larger and agreement with the experiment rotational spectrum drastically worsens. Note also that rotational bands for the superdeformed state were not yet observed in ^{254}No . Moreover, the existence of the superdeformed state as such is questionable as it is prone to be unstable against fission. Altogether, to our opinion, the coupling of "normal" and superdeformed shapes in ^{254}No is too weak to affect noticeably the low-energy spectrum. So we can safely consider only the prolate g.s. at $\beta \approx 0.3$. Following these arguments, our explanation of 0.888-MeV state as a pairing vibration seems to be the most plausible.

Recent shell-model calculations with projection after

variation [26] give in ^{254}No the $K^\pi = 0^+$ state at 0.86 MeV. However, the authors do not analyze the origin and features of the state.

Low-energy 0^+ states were earlier predicted within triaxial beyond-mean-field (TBMF) prescription in Fl ($Z=114$) [65] and Cn ($Z=112$) [58, 66] isotopes. Their excitation energies were suggested at 0.4-1.3 MeV in $^{288-292}\text{Fl}$ [65] and 0.7-2.2 MeV in $^{282-288}\text{Cn}$ [66]. Moreover, the excited 0^+ state at $E_x \approx 0.6$ MeV was experimentally observed in ^{282}Cn [58, 66] within the coincidence experiment (population of this state through α -decay from ^{286}Fl and subsequent deexcitation of the state through electron internal conversion). Perhaps, all these excited 0^+ states are also basically pairing vibrational.

Unlike Fl and Cn isotopes with Z equal or close to the suggested spherical magic number $Z=114$, our calculations concern the case of the suppressed pairing in the mid of the chain of *well deformed* nobelium isotopes whose Z and N are far from spherical magic numbers. To the best of our knowledge, previous studies of 0^+ states in well deformed nuclei did not consider the cases of the suppressed pairing.

The excited 0^+ state can serve as a sensitive indicator of the pairing in ^{254}No . It would be interesting to look for this state in the coincidence experiments like those in Refs. [58, 66]. Besides, the exploration of this state in photonuclear and (p, t) reactions could give an important information whether we indeed have a significant drop of the neutron pairing in ^{254}No . If so, then this would confirm the existence of the shell gap in the neutron s-p spectrum of this nucleus.

C. Quadrupole states $K^\pi = 2^+$

As seen in Table VI, SLy6, SkM* and SVbas give similar predictions for the energies of the first (1.58-1.70 MeV in ^{252}No and 1.31-1.45 MeV in ^{254}No) and second (1.78-2.08 MeV in ^{252}No and 1.53-1.87 MeV in ^{254}No) $K^\pi = 2^+$ states. At the same time, these forces suggest essentially different structure of the states. The first $K^\pi = 2^+$ states are γ -vibrational collective for SLy6 and SVbas in ^{252}No and for SkM* and SVbas in ^{254}No . Instead, the first 2^+ states are purely 2qp for SkM* in ^{252}No and SLy6 in ^{254}No . In most of the cases, if the first state is collective, then the next one is 2qp and vice versa. All the calculated 2^+ states lie above the observed 2^- (^{252}No) and 3^+ (^{254}No) K -isomers.

In contrast to our results, IBM calculations [29] predict first $K^\pi = 2^+$ states at much lower energies 1.09 MeV (^{252}No) and 0.94 MeV (^{254}No). The relevance of the various theoretical predictions for No isotopes can be discriminated by future experiments.

TABLE VI. Features of two lowest ($\nu=1,2$) QRPA $K^\pi = 2^+$ states in $^{252,254}\text{No}$: excitation energies E (in MeV), reduced transition probabilities $B(E22)$ (in W.u.), main 2qp components qq' , their energies $\epsilon_{qq'}$ (in MeV), contributions to the state norm $N_{qq'}$ and F-order.

Force	E	$B(E22)$	qq'	$\epsilon_{qq'}$	$N_{qq'}$	F-order
^{252}No						
SLy6	1.58	3.87	$nn[622 \downarrow, 620 \uparrow]$	2.33	0.39	F+2,F+2
			$pp[521 \downarrow, 521 \uparrow]$	2.06	0.32	F,F-2
	2.08	0.001	$pp[514 \downarrow, 521 \uparrow]$	2.06	1.00	F+1,F-2
SkM*	1.70	0.06	$pp[512 \uparrow, 521 \downarrow]$	1.61	0.99	F+3,F
	1.78	2.71	$nn[622 \uparrow, 620 \uparrow]$	2.28	0.35	F-1,F+2
SVbas	1.62	2.72	$pp[521 \uparrow, 521 \downarrow]$	1.95	0.38	F-2,F
			$nn[622 \uparrow, 620 \uparrow]$	2.48	0.29	F-1,F+2
	1.89	0.004	$pp[512 \uparrow, 521 \downarrow]$	1.86	0.99	F+3,F
^{254}No						
SLy6	1.31	0.17	$nn[622 \uparrow, 620 \uparrow]$	1.32	0.97	F-1,F+1
	1.53	3.71	$nn[622 \uparrow, 620 \uparrow]$	2.24	0.42	F-1,F+1
SkM*	1.32	2.62	$pp[521 \uparrow, 521 \downarrow]$	2.05	0.27	F-2,F
			$nn[624 \downarrow, 622 \downarrow]$	1.63	0.60	F,F+2
	1.62	0.015	$nn[622 \downarrow, 620 \uparrow]$	1.60	0.18	F+2,F+1
SVbas	1.45	4.46	$nn[622 \downarrow, 620 \uparrow]$	1.77	0.40	F+2,F+1
			$pp[521 \uparrow, 521 \downarrow]$	1.95	0.20	F-2,F
	1.87	0.32	$nn[622 \downarrow, 620 \uparrow]$	1.77	0.56	F+1,F+2
			$pp[521 \uparrow, 521 \downarrow]$	1.95	0.21	F-2,F

TABLE VII. The same as in Table VI but for $K^\pi = 3^+$. For ^{254}No , the SLy4 results are also shown.

Force	E	$B(E43)$	qq'	$\epsilon_{qq'}$	$N_{qq'}$	F-order
^{252}No						
SLy6	1.10	3.04	$pp[521 \downarrow, 514 \downarrow]$	1.16	0.99	F,F+1
	2.13	2.91	$pp[521 \downarrow, 512 \uparrow]$	2.11	0.95	F,F+3
SkM*	1.00	3.61	$pp[521 \downarrow, 514 \downarrow]$	1.05	0.97	F,F+1
	1.69	2.67	$pp[521 \downarrow, 512 \uparrow]$	1.61	0.94	F,F+3
SVbas	1.19	2.73	$pp[521 \downarrow, 514 \downarrow]$	1.21	0.98	F,F+1
	1.93	2.43	$pp[521 \downarrow, 512 \uparrow]$	1.86	0.95	F,F+3
^{254}No , $E_x=0.987$ MeV						
SLy4	1.07	3.21	$pp[521 \downarrow, 514 \downarrow]$	1.13	0.99	F,F+1
	1.74	0.67	$nn[620 \uparrow, 613 \uparrow]$	1.76	0.96	F+1,F+3
SLy6	1.11	2.41	$pp[521 \downarrow, 514 \downarrow]$	1.15	0.99	F,F+1
	1.89	1.78	$nn[620 \uparrow, 613 \uparrow]$	1.89	1.00	F+1,F+3
SkM*	1.01	3.24	$pp[521 \downarrow, 514 \downarrow]$	1.05	0.97	F,F+1
	1.41	2.15	$nn[624 \downarrow, 620 \uparrow]$	1.39	1.00	F,F+1
SVbas	1.17	3.00	$pp[521 \downarrow, 514 \downarrow]$	1.20	0.99	F,F+1
	1.87	3.28	$nn[620 \uparrow, 613 \uparrow]$	1.98	0.48	F+1,F+3
			$pp[521 \downarrow, 512 \uparrow]$	1.89	0.47	F,F+3

TABLE VIII. The same as in Table VI but for $K^\pi = 4^+$.

Force	E	$B(E44)$	qq'	$\epsilon_{qq'}$	$N_{qq'}$	F-order
^{252}No						
SLy6	1.16	$6 \cdot 10^{-4}$	$pp[521 \downarrow, 514 \downarrow]$	1.16	1.00	F,F+1
	2.11	1.78	$nn[624 \downarrow, 620 \uparrow]$	2.34	0.50	F,F+2
SkM*	1.08	0.04	$pp[521 \downarrow, 514 \downarrow]$	1.05	1.00	F,F+1
	1.85	0.37	$nn[624 \downarrow, 620 \uparrow]$	1.87	0.98	F+1,F+2
SVbas	1.22	0.04	$pp[521 \downarrow, 514 \downarrow]$	1.21	1.00	F,F+1
	2.06	0.86	$nn[624 \downarrow, 620 \uparrow]$	2.09	0.93	F,F+2
$^{254}\text{No}, E_x=1.203 \text{ MeV}$						
SLy4	1.14	0.05	$pp[521 \downarrow, 514 \downarrow]$	1.13	1.00	F,F+1
	1.77	0.002	$nn[620 \uparrow, 613 \uparrow]$	1.76	1.00	F+1,F+3
SLy6	1.16	0.07	$pp[521 \downarrow, 514 \downarrow]$	1.15	1.00	F,F+1
	1.89	10^{-4}	$nn[620 \uparrow, 613 \uparrow]$	1.89	1.00	F+1,F+3
SkM*	1.07	0.05	$pp[521 \downarrow, 514 \downarrow]$	1.05	1.00	F,F+1
	1.36	0.47	$nn[624 \downarrow, 620 \uparrow]$	1.39	0.99	F,F+1
SVbas	1.21	0.04	$pp[521 \downarrow, 514 \downarrow]$	1.20	1.00	F,F+1
	1.98	0.06	$nn[620 \uparrow, 613 \uparrow]$	1.98	0.94	F+1,F+3

D. Hexadecapole states with $K^\pi = 3^+$ and 4^+

In Table VII, the calculated features of two lowest hexadecapole $K^\pi = 3^+$ states in $^{252,254}\text{No}$ are collected. It is seen that all the applied Skyrme forces rather well describe the excitation energy $E_x=0.987$ MeV of the observed 3^+ state in ^{254}No [1, 4, 5, 8]. The first 3^+ state is purely 2qp and, in agreement with previous studies [1, 4, 5, 8, 27, 35, 37, 67], is assigned as $pp[521 \downarrow, 514 \downarrow]$. This confirms the relevance of our single-particle schemes.

For ^{252}No , our calculation also give purely 2qp 3^+ state at a similar energy 1.00-1.19 MeV and with the same assignment $pp[521 \downarrow, 514 \downarrow]$.

In Table VII, the second 3^+ state is also 2qp (with exception of SVbas case in ^{254}No). So, the impact of the hexadecapole residual interaction on 3^+ states in $^{252,254}\text{No}$ looks negligible. Instead, QPM calculations [35] predict a noticeable impact of the hexadecapole residual interaction in nobelium isotopes. Besides, a significant impact of the residual interaction was found in QPM calculations for hexadecapole states in rare-earth nuclei [63, 68].

Table VIII shows that the calculated first $K^\pi = 4^+$ states in $^{252,254}\text{No}$ have the energies and structure very similar to 3^+ states. This is not surprising since both 3^+ and 4^+ states are basically formed by the same proton 2qp configuration $pp[521 \downarrow, 514 \downarrow]$ with $|K_1 - K_2|=3$ and $K_1 + K_2=4$, respectively. This means that, near the observed 3^+ state in ^{254}No , there should be some 4^+ state. Indeed, in the recent measurements [10], a 4^+ state was observed in ^{254}No at 1.203 MeV, i.e. rather close to our predictions. In the shell-model calculations [26], the 4^+ state in ^{254}No is predicted at 1.250 MeV.

Following our calculations, a doublet $3^+, 4^+$ is expected in ^{252}No as well. In both ^{252}No and ^{254}No , the band heads 3^+ and 4^+ and corresponding rotational bands should exhibit a strong Coriolis coupling.

As shown in Table VIII, the pair $pp[521 \downarrow, 514 \downarrow]$ has a feature $B(E43) \gg B(E44)$. This is probably caused by violation in this configuration of the Nilsson selection rule $\Delta K = \Delta \Lambda$ [60, 69] for E44 transitions.

E. Octupole states with $K^\pi = 0^-, 1^-, 2^-$ and 3^-

Our results for octupole states in $^{252,254}\text{No}$ are exhibited in Table IX. The force SLy6 gives for 2^- isomer in ^{252}No the energy $E=0.946$ MeV in a good agreement with the experimental value 0.929 MeV. Instead, SLy4, SkM* and SVbas give much higher energies 1.140 (not shown), 1.462 and 1.622 MeV, respectively. In accordance with the experimental analysis [6], all the applied Skyrme forces suggest for the first 2^- state in ^{252}No the 2qp configuration $nn[734 \uparrow, 622 \uparrow]$. Following Table IX, this state demonstrates large $B(E32)$ values. In the QPM study [35], the first 2^- state is the lowest among the octupole excitations in ^{252}No . We get the same result for SLy6 but not for other forces. Altogether, SLy6 gives the most relevant description of 2^- isomer in ^{252}No .

One should mention a significant difference in SLy6 results for the lowest 2^- states in ^{252}No and ^{254}No , although in both nuclei these states are dominated by the same 2qp configuration $nn[734 \uparrow, 622 \uparrow]$. Indeed, in ^{252}No this state has a low energy 0.95 MeV and large $B(E32)=11.5$ W.u., while in ^{254}No we have the opposite picture: high energy 2.12 MeV and low $B(E32)=0.6$ W.u.. The reason of the difference in $B(E32)$ is that the transition $734 \uparrow \rightarrow 622 \uparrow$ is particle-hole in ^{252}No and hole-hole in ^{254}No (see F-order in the Table). So this transition in ^{254}No is strongly suppressed by the pairing factor $u_{qq'} = u_q v_{q'} + u_{q'} v_q$, where $u_{qq'}=0.986$ in ^{252}No and 0.077 in ^{254}No . Further, the difference in the excitation energy is caused by different neutron chemical potentials: $\lambda_n=-7.09$ MeV in ^{252}No and -6.35 MeV in ^{254}No . Note that, in our SLy6 calculations, the neutron pairing in ^{254}No is suppressed and its BCS description is rather approximate.

Our results are in accordance with recent findings for $^{252,254}\text{No}$, obtained within the cranked relativistic shell-model-like approach [24]. This study predicts the large octupole correlations (deformations) β_{32} in ^{252}No and negligible in ^{254}No .

Table IX shows that, in most of the calculations, 0^- states are more collective than 1^- states. The calculated 3^- states have low excitation energies (1.28-1.48 MeV) and the same (with exception of SLy6 in ^{254}No) dominant 2qp configuration $pp[633 \uparrow, 521 \downarrow]$.

TABLE IX. Features of the lowest QRPA octupole states with $K^\pi = 0^-, 1^-, 2^-, 3^-$ in $^{252,254}\text{No}$: excitation energies E (in MeV), reduced transition probabilities $B(E3K)$ (in W.u.), main 2qp components qq' , their energies $\epsilon_{qq'}$ (in MeV), contributions to the state norm $N_{qq'}$ and F-order.

Force	K^π	E	$B(E3K)$	qq'	$\epsilon_{qq'}$	$N_{qq'}$	F-order	K^π	E	$B(E3K)$	qq'	$\epsilon_{qq'}$	$N_{qq'}$	F-order
^{252}No														
SLy6	0^-	1.24	9.1	$pp[514 \downarrow, 633 \uparrow]$	1.35	0.93	F+1,F-1	0^-	1.25	11.2	$pp[514 \downarrow, 633 \uparrow]$	1.38	0.87	F+1,F-1
	1^-	1.41	1.5	$nn[734 \uparrow, 624 \downarrow]$	1.32	0.98	F+1,F	1^-	1.54	8.4	$nn[734 \uparrow, 613 \uparrow]$	1.78	0.82	F,F+3
	2^-	0.95	11.5	$nn[622 \uparrow, 734 \uparrow]$	1.30	0.92	F-1,F+1	2^-	2.12	0.6	$nn[622 \uparrow, 734 \uparrow]$	2.13	0.94	F-1,F
	3^-	1.35	0.1	$pp[633 \uparrow, 521 \downarrow]$	1.35	1.00	F-1,F	3^-	1.28	0.03	$nn[734 \uparrow, 622 \downarrow]$	1.213	0.94	F,F+2
SkM*	0^-	1.35	20.7	$pp[514 \downarrow, 633 \uparrow]$	1.52	0.79	F+1, F-1	0^-	1.37	16.3	$pp[514 \downarrow, 633 \uparrow]$	1.51	0.84	F+1,F-1
	1^-	1.16	2.2	$nn[734 \uparrow, 624 \downarrow]$	1.20	0.97	F,F+1	1^-	1.47	1.5	$pp[624 \uparrow, 514 \downarrow]$	1.48	0.95	F+2,F+1
	2^-	1.46	6.2	$nn[734 \uparrow, 622 \uparrow]$	1.61	0.92	F,F-1	2^-	1.80	3.7	$nn[725 \uparrow, 624 \downarrow]$	1.71	0.85	F+3,F
	3^-	1.48	0.05	$pp[633 \uparrow, 521 \downarrow]$	1.48	1.00	F-1,F	3^-	1.48	0.04	$pp[633 \uparrow, 521 \downarrow]$	1.48	1.00	F-1,F
SVbas	0^-	1.32	7.7	$pp[514 \downarrow, 633 \uparrow]$	1.42	0.92	F+1, F-1	0^-	1.30	7.4	$pp[514 \downarrow, 633 \uparrow]$	1.40	0.92	F+1,F-1
	1^-	1.71	6.1	$nn[734 \uparrow, 624 \downarrow]$	1.75	0.77	F+1,F	1^-	1.72	12.3	$nn[734 \uparrow, 613 \uparrow]$	2.03	0.42	F,F+3
				$pp[633 \uparrow, 512 \uparrow]$	2.06	0.10	F-1,F+3				$pp[633 \uparrow, 512 \uparrow]$	2.09	0.30	F-1,F+3
	2^-	1.62	12.6	$nn[734 \uparrow, 622 \uparrow]$	1.9	0.72	F+1,F-1	2^-	1.90	14.5	$pp[633 \uparrow, 521 \uparrow]$	2.15	0.44	F-1,F
	3^-	1.40	0.06	$pp[633 \uparrow, 521 \downarrow]$	1.40	1.00	F-1,F	3^-	1.39	0.05	$pp[633 \uparrow, 521 \downarrow]$	1.40	1.00	F-1,F

F. General view

The above analysis shows that the most relevant description of low-energy spectra in $^{252,254}\text{No}$ is provided by the force SLy6. So, in this section, we limit our discussion to SLy6 (and partly SLy4) results.

In Figures 5 and 6, the available experimental data [13] are compared with our SLy6 QRPA results for the lowest excited states with $K^\pi = 0^+, 2^+, 3^+, 4^+, 0^-, 1^-, 2^-, 3^-, 8^-$. The g.s. rotational bands are demonstrated. For the comparison, SLy4 results for state $K^\pi = 0^+, 2^-, 8^-$ are shown. Figures 5 and 6 display a rich spectrum of positive-parity and negative-parity states above 1 MeV in $^{252,254}\text{No}$. Note that energies of some $K > 0$ states can be 100-300 keV lower if to take into account the pairing blocking effect [35, 45]. The energies of the states in the g.s. rotational band are significantly underestimated, which is explained by too large value of the calculated moment of inertia (see Table II). So SLy6 obviously underestimates the pairing in $^{252,254}\text{No}$. SLy4 gives a more realistic description of the neutron pairing in ^{254}No and thus a better agreement for the energy of the first 0^+ state in this nucleus. Altogether, SLy6 and SLy4 results are in a reasonable agreement with available experimental data,

Further, Figure 7 shows that, aside the first multipole K^π states, the energy region $E < 2.5$ MeV can contain a lot of next (second, third, etc) QRPA states of a different collectivity. The most collective are some octupole states with $B(E3)$ of order 10-40 W.u..

The low-energy spectrum can be even richer if we consider positive-parity states with $K > 4$ and negative-parity states with $K > 3$, which were omitted in the above analysis. In Table X, the lowest proton and neu-

TABLE X. The lowest SLy6 neutron and proton 2qp configurations $K = K_1 + K_2$ and $K = |K_1 - K_2|$ in $^{252,254}\text{No}$. The configurations considered previously are underlined.

$\epsilon_{qq'}$	qq'	F-order	K_1+K_2	K_1-K_2
^{252}No				
1.16	$pp[521 \downarrow, 514 \downarrow]$	F,F+1	<u>4^+</u>	<u>3^+</u>
1.35	$pp[633 \uparrow, 514 \downarrow]$	F-1,F+1	<u>7^-</u>	<u>0^-</u>
1.35	$pp[633 \uparrow, 521 \downarrow]$	F-1,F	<u>4^-</u>	<u>3^-</u>
2.06	$pp[521 \uparrow, 521 \downarrow]$	F-2,F	<u>2^+</u>	<u>1^+</u>
2.25	$pp[521 \uparrow, 633 \uparrow]$	F-2,F-1	<u>5^-</u>	<u>2^-</u>
2.30	$pp[633 \uparrow, 512 \uparrow]$	F-1,F+3	<u>6^-</u>	<u>1^-</u>
1.30	$nn[734 \uparrow, 622 \uparrow]$	F,F-2	<u>7^-</u>	<u>2^-</u>
1.32	$nn[624 \downarrow, 734 \uparrow]$	F,F+1	<u>8^-</u>	<u>1^-</u>
2.08	$nn[624 \downarrow, 743 \uparrow]$	F,F-2	<u>7^-</u>	<u>0^-</u>
2.33	$nn[622 \uparrow, 620 \uparrow]$	F-1,F+2	<u>3^+</u>	<u>2^+</u>
2.34	$nn[624 \downarrow, 620 \uparrow]$	F,F+2	<u>4^+</u>	<u>3^+</u>
^{254}No				
1.15	$pp[521 \downarrow, 514 \downarrow]$	F,F+1	<u>4^+</u>	<u>3^+</u>
1.38	$pp[633 \uparrow, 514 \downarrow]$	F-1,F+1	<u>7^-</u>	<u>0^-</u>
1.38	$pp[633 \uparrow, 521 \downarrow]$	F-1,F	<u>4^-</u>	<u>3^-</u>
2.05	$pp[521 \uparrow, 521 \downarrow]$	F-2,F	<u>2^+</u>	<u>1^+</u>
2.27	$pp[521 \uparrow, 633 \uparrow]$	F-2,F-1	<u>5^-</u>	<u>2^-</u>
2.43	$pp[633 \uparrow, 512 \uparrow]$	F-1,F+3	<u>6^-</u>	<u>1^-</u>
1.21	$nn[734 \uparrow, 622 \downarrow]$	F,F+2	<u>6^-</u>	<u>3^-</u>
1.32	$nn[622 \uparrow, 620 \uparrow]$	F-1,F+1	<u>2^+</u>	<u>1^+</u>
1.78	$nn[734 \uparrow, 613 \uparrow]$	F,F+3	<u>8^-</u>	<u>1^-</u>
1.89	$nn[620 \uparrow, 613 \uparrow]$	F+1,F+3	<u>4^+</u>	<u>3^+</u>
2.13	$nn[622 \uparrow, 734 \uparrow]$	F-1,F	<u>7^-</u>	<u>2^-</u>
2.17	$nn[734 \uparrow, 615 \downarrow]$	F,F+5	<u>9^-</u>	<u>0^-</u>

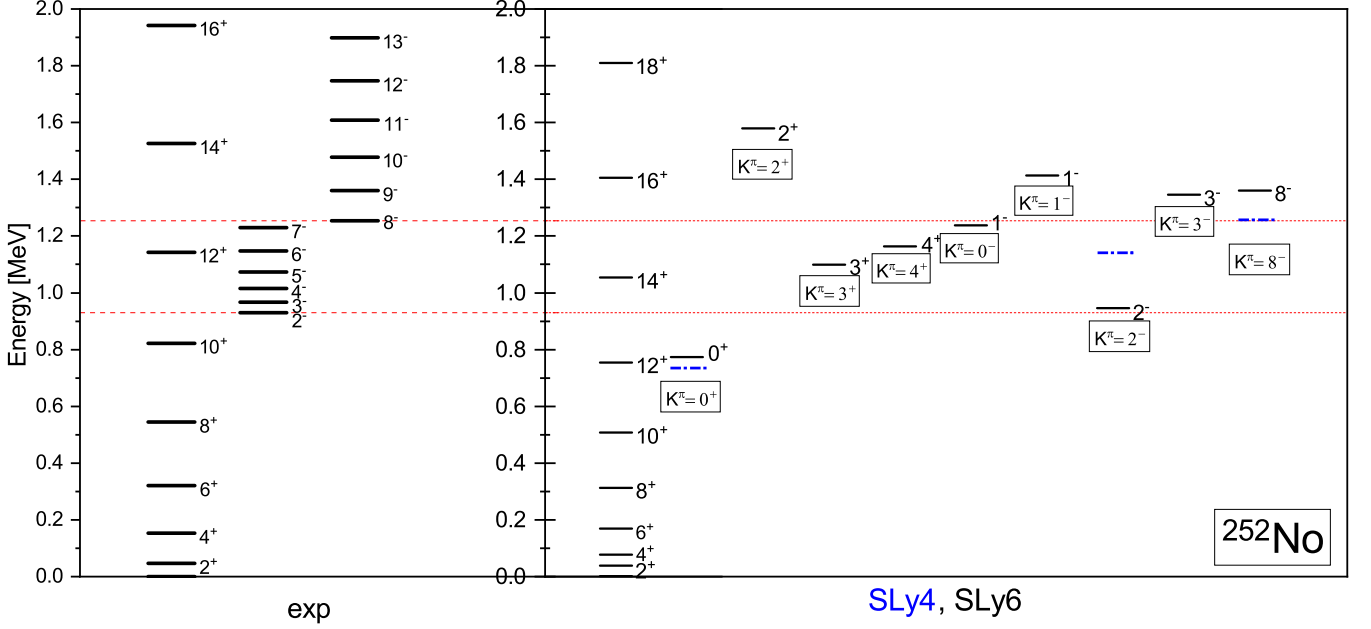


FIG. 5. Experimental [13] (left) and QRPA SLy6 and SLy4 (right) spectra in ^{252}No . The state energies are shown by black solid (SLy6) and blue dash-short (SLy4) lines. The rotational states are marked by I^π on the right. In the right panel, the band heads are marked by boxed K^π . For $K^\pi = 0^-$, the lowest $I^\pi = 1^-$ state is shown. The horizontal dashed red lines mark the experimental energies 0.929 MeV of $K^\pi = 2^-$ state and 1.254 MeV of $K^\pi = 8^-$ state.

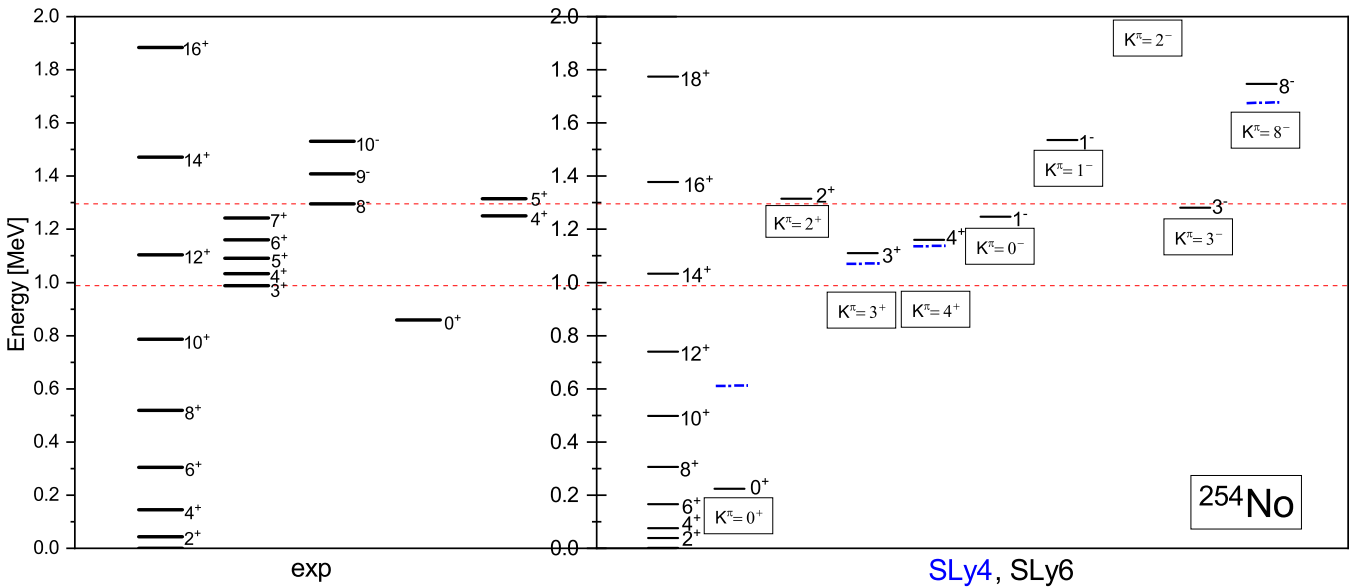


FIG. 6. The same as in fig. 5 but for ^{254}No . The horizontal dashed red lines mark the experimental energies 0.987 MeV of $K^\pi = 3^+$ state and 1.295 MeV of $K^\pi = 8^-$ state. The energy E=2.12 MeV of the lowest SLy6 $K^\pi = 2^-$ state is beyond the frame of the figure.

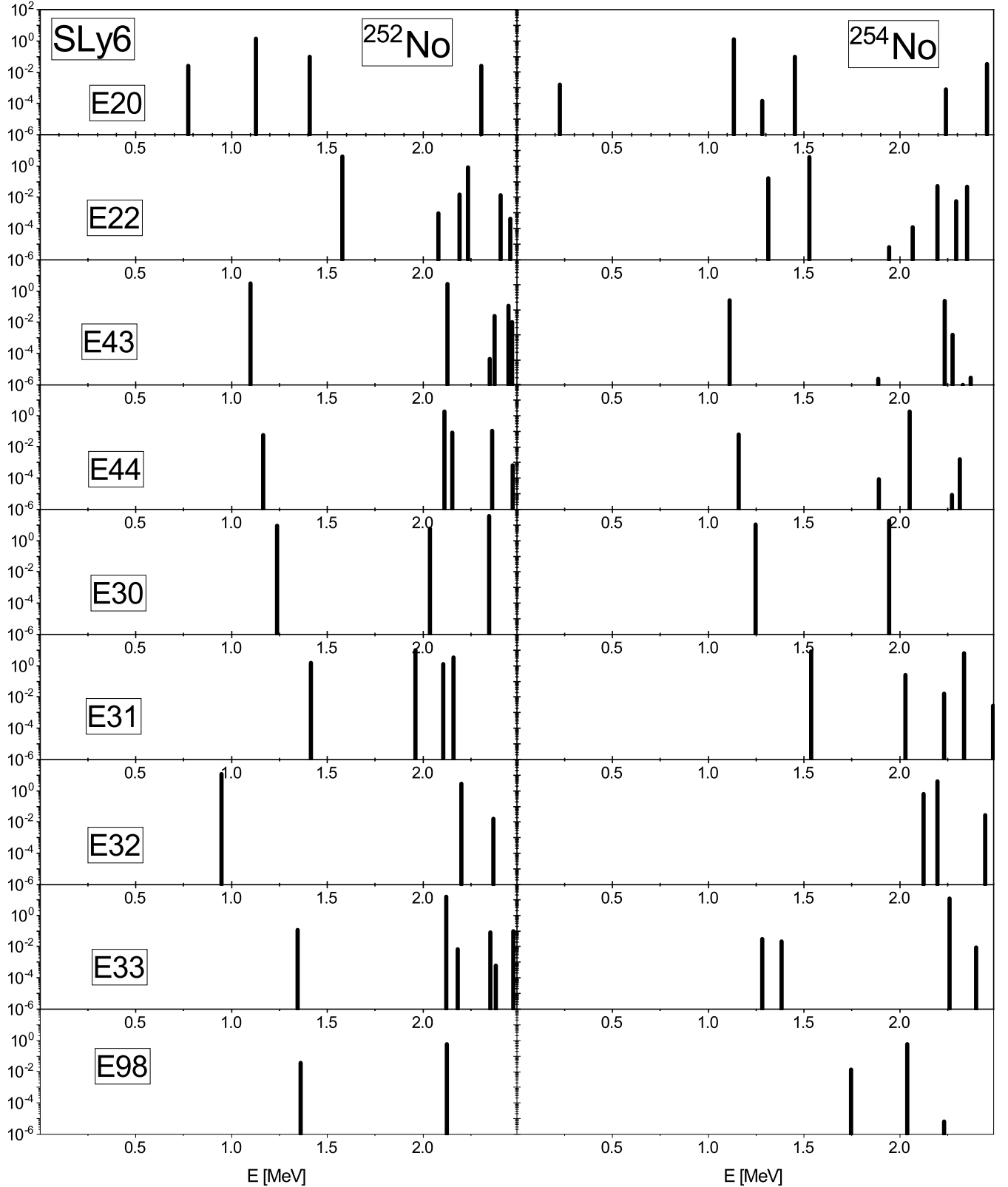


FIG. 7. SLy6 reduced transition probabilities $B(E\lambda\mu)$ (W.u. in log scale) for low-energy ($E < 2.5$ MeV) multipole QRPA states in ^{252}No and ^{254}No .

tron 2qp configurations (of particle-hole origin) for $K^\pi = 2^+, 3^+, 4^+, 0^-, 1^-, 2^-, 3^-, 8^-$ in $^{252,254}\text{No}$ are exhibited. Both possible cases $K = K_1 + K_2$ and $K = |K_1 - K_2|$ for a given 2qp configuration are considered. The K^π -values realized in the previously considered excitations are underlined.

Table X shows that, besides the states considered above, these configurations can also produce at the same excitation energies negative-parity states $K^\pi = 4^-, 5^-, 6^-, 7^-, 9^-$. In ^{252}No , 7^- states $pp[633 \uparrow, 514 \downarrow]$ and $nn[734 \uparrow, 622 \uparrow]$ should coexist at a similar low energy ≈ 1.3 MeV with 8^- isomer $nn[624 \downarrow, 734 \uparrow]$ and 2^- isomer $nn[734 \uparrow, 622 \uparrow]$. The low-energy 3^- state $pp[633 \uparrow, 521 \downarrow]$ can be accompanied by 4^- state with the similar 2qp structure. The 3^+ state $pp[521 \downarrow, 514 \downarrow]$ has 4^+ counterpart. In ^{254}No , the low-energy states 0^- and 3^- have counterparts 7^- and 4^- . The low-energy 3^+ and 4^+ states should have similar energies.

Note that counterparts with $\Delta K = 1$ can exhibit Coriolis coupling. Low-energy 2qp $K^\pi = 4^-, 5^-, 6^-, 7^-, 4^+$ configurations in ^{254}No were also predicted in self-consistent calculations with Gogny force [16].

V. CONCLUSIONS

A systematic microscopic analysis of low-energy states in even-even isotopes $^{250-262}\text{No}$ is performed within a fully self-consistent quasiparticle random-phase approximation (QRPA) method [39–41, 48]. A representative set of Skyrme forces SLy4 [42], SLy6 [42], SkM* [43] and SVbas [44] with different isoscalar effective masses m^*/m and kinds of pairing (volume and surface) is used. As compared with SLy6, the force SLy4 avoids the BCS collapse of the neutron pairing in ^{254}No and, in this sense, serves to countercheck the SLy6 results.

The low-energy excitations with $K^\pi = 0^+, 2^+, 3^+, 4^+, 0^-, 1^-, 2^-, 3^-, 8^-$ are considered. In addition, some relevant positive-parity states with $K > 4$ and negative-parity states with $K > 3$ are briefly inspected. The main attention is paid to isotopes ^{252}No and ^{254}No which possess the most extensive spectroscopic information on non-rotational states. Just for these two isotopes a significant shell gap in the neutron s-p spectrum was earlier predicted [6].

Among the applied Skyrme forces, the best performance is found for SLy6. This force rather well reproduces the energies of the observed 8^- and 2^- states in ^{252}No and 3^+ and 4^+ states in ^{254}No . Besides, SLy6 suggests a reasonable assignment $nn[734 \uparrow, 613 \uparrow]$ for disputed 8^- isomer in ^{254}No . The similar force SLy4 also demonstrates a generally good performance. As compared to SLy6, it provides a much better description of the energy of the observed $K^\pi = 0^+$ state in ^{254}No . However, SLy4 gives a worse description of the neutron mass staggering quantity $\delta_{2n}^{(3)}(N, Z)$ and of the energy of 2^- isomer in ^{252}No .

For a more accurate treatment of the pairing decrease

arising due to neutron shell gap, we also apply the forces UNEDF1 [46], UNEDF1^{SO} [28] and UNEDF2 [47], where the pairing is treated within the Lipkin-Nogami (LN) prescription. This prevents the pairing collapse. These forces are implemented for alternative description of isomeric states in ^{252}No and ^{254}No . However, despite a more realistic treatment of the pairing, the UNEDF forces do not provide a simultaneous reasonable description of $8^-, 2^-$ isomers in ^{252}No and of $3^+, 4^+$ isomers in ^{254}No . It seems that SLy6 suggests a better s-p spectrum and this factor is decisive for description of the isomers.

We assert that just a simultaneous description of well determined isomers $8^-, 2^-$ in ^{252}No and of 3^+ in ^{254}No can justify the validity of the theory. Instead, the disputed 8^- isomer in ^{254}No requires very fine tuning of the s-p spectra and pairing and, in this sense, is not so optimal for testing the theoretical models.

In accordance with the analysis [6], our SLy6 calculations predict in ^{252}No and, especially in ^{254}No , a significant shell gap (or, more precisely, a region of a low level density) in the neutron s-p spectrum and a corresponding drop of the neutron pairing. A smaller pairing drop is also obtained in SLy4 and SkM* calculations. The comparison of SLy4 and SLy6 results shows that, in the case of shell gaps, even tiny changes in the single-particle spectra can noticeably affect the pairing and related nuclear properties.

The suggested gap in the neutron s-p spectrum can have far-reaching consequences. First of all, $^{252,254}\text{No}$ should demonstrate irregularities in the features of the g.s. rotational bands (moments of inertia, $B(E2)$ -values). As the next consequence of the pairing drop, we predict in these nuclei low-energy pairing vibrational $K^\pi = 0^+$ states. Note that $K^\pi = 0^+$ state was observed at 0.888 MeV in ^{254}No [10, 11]. This state was treated as a result of coexistence of the normal deformation and superdeformation or/and coexistence of axial and triaxial shapes. Instead, our calculations show that this state should be the pairing vibration. Such low-energy 0^+ pairing vibrations are typical for rare-earth and actinide deformed nuclei [59–63].

Unlike Fl and Cn isotopes with Z equal or close to the suggested magic number $Z=114$, the nobelium isotopes perhaps exhibit a unique case of the suppressed pairing in the mid of the chain of well-deformed isotopes whose Z and N are far from the spherical magic numbers. To the best of our knowledge, previous studies of 0^+ states in heavy well deformed nuclei did not consider the cases of a suppressed pairing. Low-energy 0^+ pairing vibrations could serve as sensitive indicators of the pairing in superheavy and nearby nuclei. Following our study, they can also signal on the shell gaps. It would be interesting to investigate these states in photonuclear reactions and various γ -decay scenarios.

Our calculations show that, in $^{252,254}\text{No}$, the lowest $K^\pi = 3^+$ and 4^+ states are produced by the same 2qp configurations and so should have rather similar energies. This suggestion is confirmed by the recent observation in

^{254}No of 4^+ band head at the energy close to the energy of the previously known 3^+ isomer. Because of the similar structure, the 3^+ and 4^+ counterparts and their rotational bands should exhibit a strong Coriolis coupling.

Excitation energies and collectivity of some lowest states, e.g. $K^\pi = 2^+$, can be very different in ^{252}No and ^{254}No . The calculated octupole states also demonstrate a variety of excitation energies and 2qp/collective structures. Altogether, a rich multipole low-energy spectrum is suggested in ^{252}No and ^{254}No . In addition to octupole states, the states $K^\pi = 4^-, 7^-$ in ^{252}No and $4^-, 6^-, 7^-$ in ^{254}No are predicted.

Note that the applied Skyrme forces are characterized by different isoscalar effective masses m^*/m and so somewhat deviate in the s-p spectra, shell-gap values and pairing strength. Thus, there is a variety in predictions for low-energy 2qp and QRPA states. A further improvement of the theory is necessary. Nevertheless, even yet unperfect self-consistent methods can give reasonable interesting predictions.

Further measurements of non-rotational states in $^{252,254}\text{No}$ are very desirable. Spectroscopy of nobelium isotopes could be a crucial test for the theory pretending for description of even heavier nuclei, first of all, of superheavy elements.

ACKNOWLEDGEMENTS

V.O.N. and M.A.M. thank Dr. N.N. Arsenyev for useful discussions. A.R. acknowledges support by the Slovak Research and Development Agency under Contract No. APVV-20-0532 and by the Slovak grant agency VEGA (Contract No. 2/0175/24).

Appendix A: UNEDF1, UNEDF1^{SO} and UNEDF2 results for $^{252,254}\text{No}$.

The forces UNEDF1 [46], UNEDF1^{SO} [28] and UNEDF2 [47] (called UNEDF hereafter) in the framework of Hartree-Fock-Bogoliubov (HFB) and LN methods are applied for a more accurate description of 8^- isomer in $^{252,254}\text{No}$, where our calculations predict a weak neutron pairing. The zero-range pairing interaction (3) with $\eta=0.5$ and model parameter $\rho_{\text{pair}}=0.16 \text{ fm}^{-3}$ is used. The calculations are performed with the code [70] using the LN procedure. Note that UNEDF1^{SO} was suggested as a spectroscopic-quality force for heavy nuclei [28]. As compared with UNEDF1, in this force the spin-orbit and pairing parameters were additionally fitted to reproduce the observed spectra of heavy odd nuclei.

In Table XI we show some force parameters. It is seen that UNEDF1^{SO} spin-orbit parameters significantly deviate from UNEDF1, UNEDF2 and SLy4-SVbas values (Table I).

Table XII shows that, as compared with SLy4-SVbas set, UNEDF forces give somewhat smaller equilibrium

TABLE XI. Isoscalar effective mass m^*/m , proton and neutron pairing constants G_p and G_n , IS and IV spin-orbit parameters b_4 and b'_4 for UNEDF1, UNEDF1^{SO}, and UNEDF2.

	UNEDF1	UNEDF1 ^{SO}	UNEDF2
m^*/m	0.99	1.07	0.99
G_p (MeV fm ³)	206.58	230.33	253.30
G_n (MeV fm ³)	186.07	208.89	192.1
b_4 (MeV fm ⁵)	38.4	25.7	96.508
b'_4 (MeV fm ⁵)	71.3	77.3	-16.916

TABLE XII. Quadrupole deformation β , proton and neutron pairing gaps without and with LN addition λ_2 in $^{252,254}\text{No}$, calculated with UNEDF1, UNEDF1^{SO} and UNEDF2.

	UNEDF1	UNEDF1 ^{SO}	UNEDF2
^{252}No			
β	0.287	0.285	0.283
Δ_p (MeV)	0.320	0.540	0.401
$\Delta_p + \lambda_{2p}$ (MeV)	0.487	0.730	0.592
Δ_n (MeV)	0.375	0.424	0.464
$\Delta_n + \lambda_{2n}$ (MeV)	0.561	0.608	0.672
^{254}No			
β	0.285	0.282	0.280
Δ_p (MeV)	0.318	0.534	0.402
$\Delta_p + \lambda_{2p}$ (MeV)	0.485	0.724	0.594
Δ_n (MeV)	0.371	0.418	0.459
$\Delta_n + \lambda_{2n}$ (MeV)	0.555	0.611	0.664

quadrupole deformations in $^{252,254}\text{No}$. Since LN procedure is used, we avoid the collapse of the neutron pairing in ^{254}No . Moreover, here UNEDF1 and UNEDF2 provide the neutron pairing stronger than the proton one.

In Table XIII, we show the calculated lowest neutron and proton 2qp $K^\pi = 8^-$ excitations in $^{252,254}\text{No}$. In the simple case of ^{252}No , only one neutron and one proton 2qp pairs are listed. In a more complicated case of ^{254}No , three lowest configurations are demonstrated for each force. The lowest 2qp pair is considered as a priority candidate for the observed 8^- isomer.

TABLE XIII. The energies (in MeV) of the lowest neutron and proton 2qp 8^- states in $^{252,254}\text{No}$, calculated with UNEDF1, UNEDF1^{SO} and UNEDF2.

	UNEDF1	UNEDF1 ^{SO}	UNEDF2
$^{252}\text{No}, E_x = 1.254 \text{ MeV}$			
$nn[624 \downarrow, 734 \uparrow]$	0.870	0.954	1.119
$pp[624 \uparrow, 514 \downarrow]$	1.242	1.279	1.430
$^{254}\text{No}, E_x = 1.295 \text{ MeV}$			
$nn[624 \downarrow, 734 \uparrow]$	1.036	1.141	1.338
$nn[613 \uparrow, 734 \uparrow]$	1.081	1.321	1.605
$pp[624 \uparrow, 514 \downarrow]$	1.190	1.250	1.390

TABLE XIV. Experimental and calculated energies (in MeV) of $K^\pi = 2^-$ isomer $nn[622 \uparrow, 734 \uparrow]$ in ^{252}No and 3^+ isomer $pp[521 \downarrow, 514 \downarrow]$ in ^{254}No .

	exper	UNEDF1	UNEDF1 ^{SO}	UNEDF2
2^- in ^{252}No	0.929	0.991	1.141	1.207
3^+ in ^{254}No	0.987	0.695	1.168	0.880

We see that, in agreement with our SLy4-SVbas results (Table IV), UNEDF forces also suggest for 8^- isomer in ^{252}No the neutron configuration $nn[624 \downarrow, 734 \uparrow]$. However, for all three UNEDF forces, the energy of 8^- isomer is significantly underestimated. Note that the present UNEDF calculations do not take into account the pairing blocking effect which should additionally downshift the calculated isomer energy.

In ^{254}No , UNEDF forces provide a better description of the isomer energy than the best SLy4, SLy6 and SkM* cases shown in Table IV. Instead of SLy4 and SLy6 assignment $nn[613 \uparrow, 734 \uparrow]$, UNEDF forces suggest the configuration $nn[624 \downarrow, 734 \uparrow]$. Note that the energy interval between these two neutron configurations is rather

small (especially for UNEDF1 and UNEDF1^{SO}) and so this UNEDF assignment is rather tentative. To our opinion, what is indeed important is that UNEDF forces do not provide a *simultaneous* description of the energies of both 8^- isomers in ^{252}No and ^{254}No .

In ^{254}No , the energy intervals between the lowest neutron and proton 2qp configurations are also small: 164, 109 and 52 keV for UNEDF1, UNEDF1^{SO} and UNEDF2, respectively. These values are comparable with collective shifts due to $\lambda\mu=98$ residual interaction (see discussion in Sec. IV-A). So, in principle, 8^- isomer ^{254}No can be a mixture of neutron and proton 2qp pairs.

Finally, Table XIV shows that UNEDF forces do not provide a simultaneous description of $K^\pi = 2^-$ isomer $nn[622 \uparrow, 734 \uparrow]$ in ^{252}No and $K^\pi = 3^+$ isomer $pp[521 \downarrow, 514 \downarrow]$ in ^{254}No (though perhaps the UNEDF1^{SO} results can be downshifted to the proper values due to the pairing blocking effect). At the same time, as shown in Tables VII and IX, we get a good description of these isomers with SLy6. Altogether, one may conclude, that the *simultaneous* description of isomeric states in $^{252,254}\text{No}$ with UNEDF forces is generally not good. At least, it is not better than in SLy4, SLy6 and SkM* cases. The best general performance is demonstrated by SLy6 force.

[1] R.-D. Herzberg and P.T. Greenlees, In-beam and decay spectroscopy of transfermium nuclei, *Prog. Part. Nucl. Phys.* **61**, 674 (2008).

[2] F.P. Heßberger, K isomers in transuranium nuclei, arXiv:2309.10468v2[nucl-ex].

[3] D. Ackermann, Decay spectroscopy of heavy and superheavy nuclei, arXiv:2501.04053v4[nucl-ex].

[4] R.-D. Herzberg et al, Nuclear isomers in superheavy elements as stepping stones towards the island of stability, *Nature* **442**, 896 (2006).

[5] S.K. Tandel et al, K isomers in ^{254}No : probing single-particle energies and pairing strengths in the heaviest nuclei, *Phys. Rev. Lett.* **97**, 082502 (2006).

[6] A. P. Robinson et al, $K^\pi=8^-$ isomers and $K^\pi=2^-$ octupole vibrations in $N=150$ shell-stabilized isotones, *Phys. Rev. C* **78**, 034308 (2008).

[7] F.P. Hessberger et al, Decay studies of K isomers in ^{254}No , *Eur. Phys. J. A* **43**, 55 (2010).

[8] R.M. Clark et al, High-K multi-quasiparticle states in ^{254}No , *Phys. Lett. B* **690**, 19 (2010).

[9] M.S. Tezekbayeva et al, Study of the production and decay properties of neutron-deficient nobelium isotopes, *Eur. Phys. J. A* **58**, 52 (2022).

[10] M. Forge et al, New results on the decay spectroscopy of ^{254}No with GABRIELA@SHELS, *Journal of Physics: Conference Series* **2586**, 012083 (2023).

[11] M. Forge, Ph.D. thesis, Étude des états isomériques des noyaux dits superlourds cas du ^{254}No . Physique Atomique [physics.atom-ph], University of Strasbourg, 2023, <https://theses.hal.science/tel-04397507v1>.

[12] S. G. Wahid et al, Isomers and hindrances in ^{254}No : A touchstone for theories of superheavy nuclei, *Phys. Rev. C* **111**, 034320 (2025).

[13] National Nuclear Data Center (NNDC) <http://www.nndc.bnl.gov/nudat3>.

[14] A. Baran, Z. Lojewski, K. Sieja, and M. Kowal, Global properties of even-even superheavy nuclei in macroscopic-microscopic models, *Phys. Rev. C* **72**, 044310 (2005).

[15] W. Kleinig, V. O. Nesterenko, J. Kvasil, P.-G. Reinhard, and P. Vesely, Description of the dipole giant resonance in heavy and superheavy nuclei within Skyrme random-phase approximation, *Phys. Rev. C* **78**, 044313 (2008).

[16] J.-P. Delaroche, M. Girod, H. Goutte, and J. Libert, Structure properties of even-even actinides at normal and super deformed shapes analysed using the Gogny force, *Nucl. Phys. A* **771**, 103 (2006).

[17] A.V. Afanasjev, T.L. Khoo, S. Frauendorf, G.A. Lalazissis, and I. Ahmad, Cranked relativistic Hartree-Bogoliubov theory: Probing the gateway to superheavy nuclei, *Phys. Rev. C* **67**, 024309 (2003).

[18] A.V. Afanasjev and O. Abdurazakov, Pairing and rotational properties of actinides and superheavy nuclei in covariant density functional theory, *Phys. Rev. C* **88**, 014320 (2013).

[19] J. Dobaczewski, A.V. Afanasjev, M. Bender, L.M. Robledo, and Yue Shi, Properties of nuclei in the nobelium region studied within the covariant, Skyrme, and Gogny energy density functionals, *Nucl. Phys. A* **944**, 388 (2015).

[20] D. Vretenar, A.V. Afanasjev, G.A. Lalazissis, and P. Ring, Relativistic Hartree-Bogoliubov theory: static and dynamic aspects of exotic nuclear structure, *Phys. Rep.* **409**, 101 (2005).

[21] M. Bender, P.-H. Heenen, and P.-G. Reinhard, Self-consistent mean-field models for nuclear structure, *Rev. Mod. Phys.* **75**, 121 (2003).

[22] S. Perú and M. Martini, Mean field based calculations with the Gogny force, *Eur. Phys. J. A* **50**, 88 (2014).

[23] Yuxin Guo and Yue Shi, Stabilization for deformed superheavy nuclei: A shell correction analysis, *Phys. Rev. C* **110**, 054314 (2024).

[24] F.F. Xu, Y.K. Wang, Y.P. Wang, P. Ring, and P.W. Zhao, Emergence of high-order deformation in rotating transfermium nuclei: A microscopic understanding, *Phys. Rev. Lett.* **133**, 022501 (2024).

[25] Zhen-Hua Zhang, Xiao-Tao He, Jin-Yan Zeng, En-Guang Zhao, and Shan-Gui Zhou, Systematic investigation of the rotational bands in nuclei with $Z \approx 100$ using a particle-number conserving method based on a cranked shell model, *Phys. Rev. C* **85**, 014324 (2012).

[26] D.D. Dao and F. Nowacki, Nuclear structure within a discrete nonorthogonal shell model approach: New frontiers, *Phys. Rev. C* **105**, 054314 (2022).

[27] D.D. Dao and F. Nowacki, First complete description of low-lying spectroscopy in ^{254}No , arXiv:2409.08210v3[nucl-th] (2025).

[28] Yue Shi, J. Dobaczewski, and P.T. Greenlees, Rotational properties of nuclei around ^{254}No investigated using a spectroscopic-quality Skyrme energy density functional, *Phys. Rev. C* **89**, 034309 (2014).

[29] A. D. Efimov and I. N. Izosimov, High-spin states of yrast bands in even Pu, Cm, Fm, and No isotopes, *Phys. Atom. Nucl.* **84**, 660 (2021).

[30] E.V. Mardyban, T.M. Shneidman, E.A. Kolganova, and R.V. Jolos, Manifestation of reflection-asymmetric deformation in the structure of superheavy nuclei, *Phys. Part. Nucl. Lett.* **19**, 646 (2022).

[31] T.M. Shneidman, G.G. Adamian, N.V. Antonenko, and R.V. Jolos, Possible alternative parity bands in the heaviest nuclei, *Phys. Rev. C* **74**, 03 4316 (2006).

[32] F.L. Bello Garrotea et al, Experimental observation of the M1 scissors mode in ^{254}No , *Phys. Lett. B* **834**, 137479 (2022).

[33] E.B. Balbutsev and I.V. Molodtsova, Scissors mode in transuranium elements, *Eur. Phys. J. A* **60**, 185 (2024).

[34] V.G. Soloviev, A.V. Sushkov, and A.Yu. Shirikova, Description of Nonrotational States of ^{250}Cf and ^{256}Fm , *Sov. J. Nucl. Phys.* **54**, 748 (1991).

[35] R.V. Jolos, L.A. Malov, N.Yu. Shirikova and A.V. Sushkov, Structure of some low lying two-quasiparticle and collective states in nuclei with $Z \approx 100$ considered in the quasiparticle phonon model, *J. Phys. G: Nucl. Part. Phys.* **38**, 115103 (2011).

[36] G.G. Adamian, N.V. Antonenko, and W. Scheid, High-spin isomers in some of the heaviest nuclei: Spectra, decays, and population, *Phys. Rev. C* **81**, 024320 (2010).

[37] Xiao-Tao He, Shu-Young Zhao, Zhen-Hua Zhang, and Zhong-Zhou Ren, High-K multi-particle bands and pairing reduction in ^{254}No , *Chinese Phys. C* **44**, 034106 (2020).

[38] J. Zang, H.-Q. Zhang, T.M. Shneidman, R.V. Jolos, and X.-T. He, Influences of $Z=100$ and $N=152$ deformed shells on $K^\pi = 8^-$ isomers and rotational bands in $N=150$ isotones, *Phys. Rev. C* **111**, 014319 (2025).

[39] A. Repko, J. Kvasil, V.O. Nesterenko, and P.-G. Reinhard, Skyrme RPA for spherical and axially symmetric nuclei, arXiv:1510.01248 nucl-th, (2015).

[40] A. Repko, J. Kvasil, V.O. Nesterenko, and P.-G. Reinhard, Pairing and deformation effects in nuclear excitation spectra, *Eur. Phys. J. A* **53**, 221 (2017).

[41] J. Kvasil, A. Repko, and V. O. Nesterenko, Elimination of spurious modes before the solution of quasiparticle random-phase-approximation equations, *Eur. Phys. J. A* **55**, 213 (2019).

[42] E. Chabanat, P. Bonche, P. Haensel, J. Meyer, and R. Schaeffer, A Skyrme parametrization from subnuclear to neutron star densities Part II. Nuclei far from stabilities, *Nucl. Phys. A* **35**, 231 (1998).

[43] J. Bartel, P. Quentin, M. Brack, C. Guet, and H.-B. Hakansson, Towards a better parametrisation of Skyrme-like effective forces: A critical study of the SkM force, *Nucl. Phys. A* **386**, 79 (1982).

[44] P. Klüpfel, P.-G. Reinhard, T. J. Burvenich, and J. A. Maruhn, Variations on a theme by Skyrme: A systematic study of adjustments of model parameters, *Phys. Rev. C* **79**, 034310 (2009).

[45] V.O. Nesterenko, V.G. Kartavenko, W. Kleinig, J. Kvasil, A. Repko, R.V. Jolos, and P.-G. Reinhard, Skyrme random-phase-approximation description of lowest $K^\pi = 2_1^+$ states in axially deformed nuclei, *Phys. Rev. C* **93**, 034301 (2016).

[46] M. Kortelainen, J. McDonnell, W. Nazarewicz, P.-G. Reinhard, J. Sarich, N. Schunck, M.V. Stoitsov, and S.M. Wild, *Phys. Rev. C* **85**, 024304 (2012).

[47] M. Kortelainen, J. McDonnell, W. Nazarewicz, E. Olsen, P.-G. Reinhard, J. Sarich, N. Schunck, S.M. Wild, D. Davesne, J. Erler, and A. Pastore, *Phys. Rev. C* **89**, 054314 (2014).

[48] P.-G. Reinhard, B. Schuetrumpf, and J.A. Maruhn, The Axial Hartree-Fock + BCS Code SkyAx, *Comp. Phys. Communic.* **258**, 107603 (2021).

[49] M. Bender, K. Rutz, P.-G. Reinhard, and J.A. Maruhn, Pairing gaps from nuclear mean-field models, *Eur. Phys. J. A* **8**, 59 (2000).

[50] P.-G. Reinhard, private communication.

[51] D.J. Thouless and J.G. Valatin, Time-dependent Hartree-Fock equations and rotational states of nuclei, *Nucl. Phys.* **31**, 211 (1962).

[52] A. Bohr and B.R. Mottelson, *Nuclear Structure*, Vol. II, (World Scientific, Singapore, 1998).

[53] Meng Wang, W.J. Huang, F.G. Kondev, G. Audi, and S. Naimi, The AME 2020 atomic mass evaluation (II). Tables, graphs and references, *Chinese Phys. C* **45**, 030003 (2021).

[54] HuaLei Wang, HongLiang Liu, FuRong Xu, and ChangFeng Jiao, Investigation of octupole effects in superheavy nuclei with improved potential-energy-surface calculations, *Chinese Science Bulletin*, **57**, 1761 (2012).

[55] S.G. Nilsson, *Mat. Fys. Medd. Dan. Vid. Selsk.* **29**, n.16 (1965).

[56] B. Sulignano et al, Identification of a K isomer in ^{252}No , *Eur. Phys. J. A* **33**, 327 (2007).

[57] N.K. Kuzmenko, V.M. Mikhailov, and V.O. Nesterenko, Pairing in multi-quasiparticle states, *Bull. Acad. Sci. USSR, Phys. Ser.* **50**, 41 (1986).

[58] A. Samark-Roth et al, Spectroscopy along flerovium decay chains. III. Details on experiment, analysis, ^{282}Cn , and spontaneous fission branches, *Phys. Rev. C* **107**, 024301 (2023).

[59] E.P. Grigorjev and V.G. Soloviev, *Structure of even deformed nuclei* (Nauka, Moscow, 1974).

[60] V.G. Soloviev, *Theory of Atomic Nuclei* (Pergamon Press, Oxford, 1976).

[61] V.G. Soloviev, A.V. Sushkov, and N.Yu. Shirikova, Low-

lying nonrotational states in well deformed even-even nuclei in the rare-earth region, *Phys. Part. Nucl.* **27**, 1643 (1996).

[62] N. Lo Iudice, A.V. Sushkov, and N.Yu. Shirikova, Microscopic structure of low-lying 0^+ states in deformed nuclei, *Phys. Rev. C* **72**, 034303 (2005).

[63] N. Lo Iudice and A.V. Sushkov, Microscopic structure of low-lying states in $^{188,190,192}\text{Os}$, *Phys. Rev. C* **78**, 054304 (2008).

[64] J.L. Egido and L.M. Robledo, "Fission barriers at high angular momentum and the ground state rotational band of the nucleus ^{254}No ", *Phys. Rev. Lett.* **85**, 6 (2000).

[65] J.L. Egido and A. Jungclaus, Predominance of triaxial shapes in transitional super-heavy nuclei: Ground-state deformation and shape coexistence along the Flerovium ($Z=114$) chain of isotopes, *Phys. Rev. Lett.* **125**, 192504 (2020).

[66] A. Samark-Roth et al, Spectroscopy along Flerovium decay chains: Discovery of ^{280}Ds and an excited state in ^{282}Cn , *Phys. Rev. Lett.* **126**, 032503 (2021).

[67] H.L. Liu, F.R. Xu, P.M. Walker, and C.A. Bertulani, Effects of high-order deformation on high-K isomers in superheavy nuclei, *Phys. Rev. C* **83**, 011303(R) (2011).

[68] V.O. Nesterenko, V.G. Soloviev, A.V. Sushkov, and N.Yu. Shirikova, Hexadecapole states in deformed nuclei, *Sov. J. Nucl. Phys.* **44**, n.6, 938 (1986).

[69] B. Mottelson and S.G. Nilsson, *Mat. Fys. Skr. Dan. Vid. Selsk* **1**, n.8 (1959).

[70] M.V. Stoitsov, N. Schunck, M. Kortelinen, N. Michel, H. Nam, E. Olsen, J. Sarich, and S. Wild, Axially deformed solution of the Skyrme-Hartree-Fock-Bogoliubov equations using the transformed harmonic oscillator basis (II) HFBTHO v2.00d: A new version of the program, *Comp. Phys. Comm.* **184**, 1592 (2013).